INFORMATION TO USERS

This reproduction was made from a copy of a manuscript sent to us for publication and microfilming. While the most advanced technology has been used to photograph and reproduce this manuscript, the quality of the reproduction is heavily dependent upon the quality of the material submitted. Pages in any manuscript may have indistinct print. In all cases the best available copy has been filmed.

The following explanation of techniques is provided to help clarify notations which may appear on this reproduction.

1. Manuscripts may not always be complete. When it is not possible to obtain missing pages, a note appears to indicate this.

2. When copyrighted materials are removed from the manuscript, a note appears to indicate this.

3. Oversize materials (maps, drawings, and charts) are photographed by sectioning the original, beginning at the upper left hand corner and continuing from left to right in equal sections with small overlaps. Each oversize page is also filmed as one exposure and is available, for an additional charge, as a standard 35mm slide or in black and white paper format.*

4. Most photographs reproduce acceptably on positive microfilm or microfiche but lack clarity on xerographic copies made from the microfilm. For an additional charge, all photographs are available in black and white standard 35mm slide format.*

***For more information about black and white slides or enlarged paper reproductions, please contact the Dissertations Customer Services Department.**

Hibbard, John Arthur

A HIGH VOLTAGE D.C. PULSE SYSTEM AND ASSOCIATED ATHERMAL, IN VITRO EXPERIMENTS

The University of Arizona M.S. 1986

PLEASE NOTE:

In all cases this material has been filmed in the best possible way from the available copy. Problems encountered with this document have been identified here with a check mark __✓__.

1. Glossy photographs or pages __✓__
2. Colored illustrations, paper or print _____
3. Photographs with dark background __✓__
4. Illustrations are poor copy _____
5. Pages with black marks, not original copy _____
6. Print shows through as there is text on both sides of page _____
7. Indistinct, broken or small print on several pages __✓__
8. Print exceeds margin requirements _____
9. Tightly bound copy with print lost in spine _____
10. Computer printout pages with indistinct print _____
11. Page(s) _____ lacking when material received, and not available from school or author.
12. Page(s) _____ seem to be missing in numbering only as text follows.
13. Two pages numbered _____. Text follows.
14. Curling and wrinkled pages _____
15. Dissertation contains pages with print at a slant, filmed as received _____
16. Other _____

_____

_____

University
Microfilms
International

A HIGH VOLTAGE D.C. PULSE SYSTEM

AND

ASSOCIATED ATHERMAL, IN VITRO EXPERIMENTS

by

John Arthur Hibbard

A Thesis Submitted to the Faculty of the

DEPARTMENT OF ELECTRICAL AND COMPUTER ENGINEERING

In Partial Fulfillment of the Requirements
For the Degree of

MASTER OF SCIENCE
WITH A MAJOR IN ELECTRICAL ENGINEERING

In the Graduate College

THE UNIVERSITY OF ARIZONA

1 9 8 6

STATEMENT BY AUTHOR

This thesis has been submitted in partial fulfillment of requirements for an advanced degree at The University of Arizona and is deposited in the University Library to be made available to borrowers under rules of the Library.

Brief quotations from this thesis are allowable without special permission, provided that accurate acknowledgment of source is made. Requests for permission for extended quotation from or reproduction of this manuscript in whole or in part may be granted by the head of the major department or the Dean of the Graduate College when in his or her judgment the proposed use of the material is in the interests of scholarship. In all other instances, however, permission must be obtained from the author.

SIGNED: John Arthur Hibbard

APPROVAL BY THESIS DIRECTOR

This thesis has been approved on the date shown below:

Roger C. Jones

Roger C. Jones
Professor of Electrical
and Computer Engineering

April 16, 1986
Date

ACKNOWLEDGMENTS

In a cross-discipline work as this there are several people that deserve acknowledgment. Foremost is my advisor, Dr. R. C. Jones, for his support and guidance. Bob Randles and Joe Bartholomeaux, from the University of Arizona Department of Physical Resources, constructed the pulse system and provided important input during its design. I wish to extend special thanks to Dr. G. T. Bowden, from the University of Arizona Health Sciences Center Department of Radiation-Oncology, and the members of his research group for the generous use of their laboratory. Without their assistance, the biological work could not have been performed. A word of thanks is also due to Sally Adams who carefully typed and formatted the final version of this manuscript. Finally, I am indebted to my wife Anna who provided love and encouragement throughout this endeavor.

TABLE OF CONTENTS

TABLE OF CONTENTS--Continued

LIST OF ILLUSTRATIONS

LIST OF ILLUSTRATIONS--Continued

LIST OF TABLES

ABSTRACT

Mouse leukemia L1210 cells were subjected to short, high power DC pulses. The pulse duration was 40 nanoseconds, and the electric field strength, in the parallel plate cell holder, ranged from 11 KV/cm to 15 KV/cm. The maximum number of pulses was 35,000, yielding a 1.1°C temperature rise in the medium. No statistically significant effect upon cell survival was obtained with pulsing alone. Experiments testing for synergism between pulsing and exposure to cis-diaminedichloroplatinum (II) (cis-DDP) were also performed. When the cells were pulsed for one hour prior to cis-DDP exposure, a significant decrease in cell survival, relative to the cis-DDP control cell survival, was observed. The 99% confidence interval for the cis-DDP control was 46% to 60% (percent survival), whereas the 99% confidence interval for the cells pulsed prior to cis-DDP exposure was 25% to 29%.

CHAPTER 1

INTRODUCTION

The purpose of this thesis was to continue the work of Dr. Roger C. Jones, which was started while on sabbatical leave in Denmark, during 1982 and 1983. His work there consisted of treating cancerous cells with high voltage, DC pulse electric fields, and then determining the effects of this treatment through the use of biological experiments. His equipment generated pulses having a width of 0.75 nanoseconds and a pulse repetition rate of approximately 4 Hz. The results of his experiments indicated that those fields had no noticeable effect upon the cells. My intent was to construct a DC pulse system which generated a greater pulse width and a higher electric field, with the expectation of obtaining positive treatment results.

Chapter Two describes the construction of the pulse system. A square coaxial transmission line, six meters in length, was constructed and used to form 40 nanosecond pulses. (The transmission line is charged, using a 50 KV DC power supply, and then discharged across a spark gap. The spark gap spacing can be changed, thus allowing a variable pulse repetition frequency of 2-5 Hz.) The characteristic impedance of the transmission line was calculated, and then

the pulse system was analyzed assuming a matched termination. Figure 1.1 shows a photograph of the square coaxial transmission line.

A parallel-plate cell holder was used to contain the cell solution during treatment. Chapter Three discusses the design of this holder. The transmission line is terminated in the cell holder; thus, it was designed to have an overall impedance (when filled with cell solution) which matched the characteristic impedance of the line as closely as possible. The design involved altering the cell holders used by Dr. Jones. The characteristic impedance of the transmission line in his system was lower than that of the present system; therefore, the geometry of the cell holder was altered to increase its overall filled impedance. Figure 1.2 shows a photograph of the pulse system front end, including the cell holder.

Chapter Four presents an analysis of the pulse system. Initially, the pulse formation is described assuming a matched termination, then, it is analyzed for the actual mismatched case. A frequency domain analysis is presented for the mismatched case. This analysis is then compared to that of an ideal pulse. The chapter concludes with a discussion of signal power and energy.

In Chapter Five, the actual impedance of the filled cell holder is determined by measurements with a RF Vector

Figure 1.1. Square coaxial transmission line.

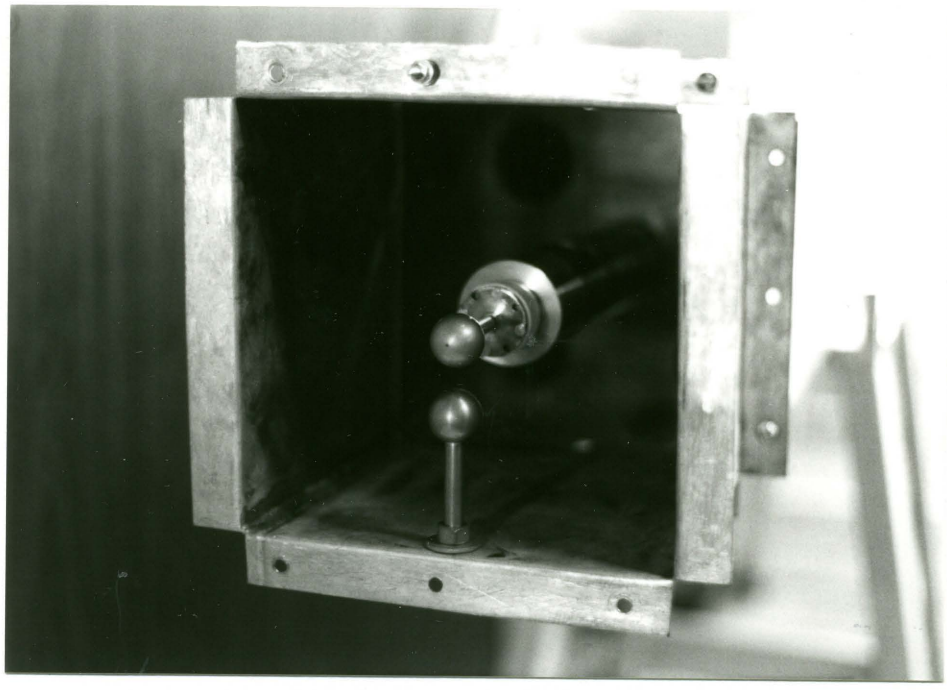

Figure 1.2. Pulse system front end, including the parallel-plate cell holder.

Impedance meter. The reason for this experimental value differing from the calculated value (given in Chapter Three) is discussed in the section on Medium Conductivity. The electric field within the cell holder, resulting from the mismatched termination, is then calculated. A graph of the electric field versus the pulse repetition frequency (PRF) is given in Figure 5.1. During each experiment the PRF is determined. The approximate electric field, in the cell holder, for each experiment, can then be found using this graph. The cell holder analysis concludes with a discussion of energy deposition and related temperature rise.

Chapter Six presents the biological procedures used, the experiments performed, and the results obtained. The cells used for the experiments are from the mouse leukemia L1210 cell line. All aspects of maintaining the cell line were described; these included medium preparation, contamination testing and subculturing procedures. The experimental end point analyzed was cell survival. The procedures for analyzing cell survival (assaying in soft agar) were also given. Three different sets of experiments were carried out. The cell holders were tested for toxicity, and the methods used in transporting cell solutions from the hospital, to the Quantum Electronics Laboratory, and back to the hospital, were tested for contamination. Once the cell holders were found to be nontoxic, and contamination-free

transportation methods were devised, the pulse experiments were performed. In addition to pulsing, experiments checking for the possibility of synergism between pulsing and exposure to a chemotherapeutic drug were carried out. The drug chosen was cis-diaminedichloroplatinum (II), available commercially under the name Platinol. For completeness, a brief discussion of Platinol's indications and adverse reactions has been included.

Chapter Seven presents the conclusions. The results are summarized, and their significance is discussed. In addition, some possibilities for future experimentation, including in vivo cases, are given. The thesis concludes with a brief discussion of some advances, already obtained, from pulsed electric field research.

This work was intended for two audiences, those in electrical engineering, and those in the biological fields. As such, some of the engineering material may appear, to those in the engineering field, to be presented in a somewhat elementary fashion. Likewise, some of the biological material may seem elementary to those more experienced in that field. The presentation of the material in this manner was intentional. This was believed to be the best way to maximize comprehension in both audiences.

CHAPTER 2

PULSE SYSTEM DESIGN AND OPERATION

Pulse System Design

The DC pulse system consists of a 50 KV DC power supply, a 500 M ohm series resistance and a terminated square coaxial transmission line six meters in length. A spark gap is used to discharge the system. Figure 2.1 shows a schematic representation of the pulse system.

The pulse width is constrained by the length of the transmission line, and the pulse repetition frequency is determined by the total charge on the line and the spark gap spacing.

Originally a high voltage heliax line was to be used for the transmission line, but due to financial considerations it was decided that the transmission line should be fabricated. Copper pipe having a 2 1/4 inch outer diameter was used as the inner conductor, due to its availability. The outer conductor was constructed from heavy gauge galvanized steel.

A square configuration was decided on for structural reasons. Because the transmission line was designed to be six meters in length, it was decided that it would be made in three sections, each two meters in length, allowing it to

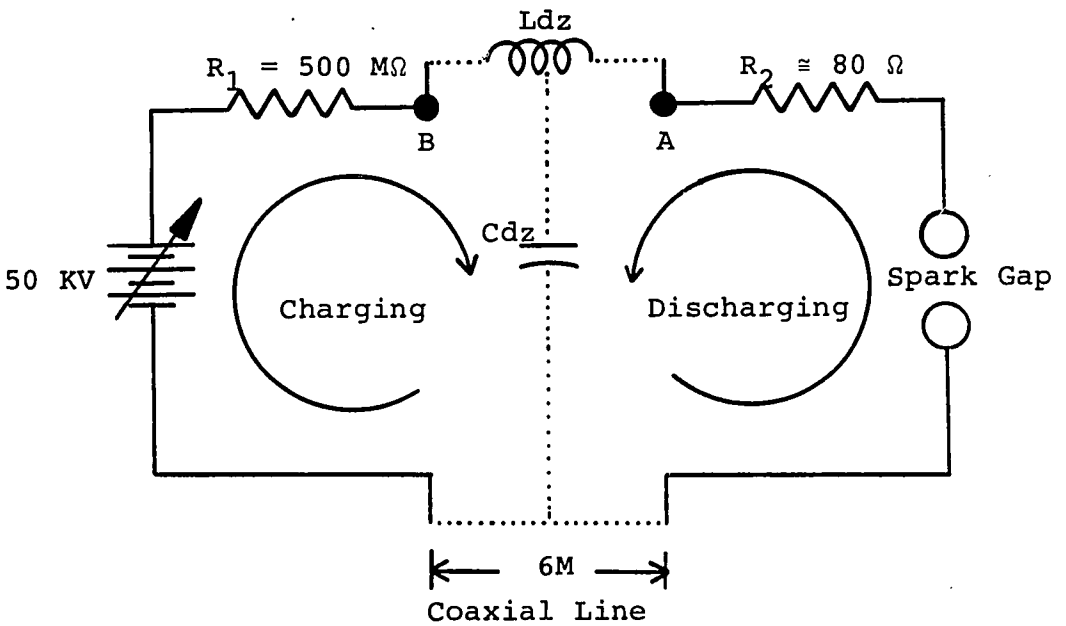

Figure 2.1. Equivalent pulse system circuit.

be brought down a staircase leading into the Quantum Electronics Laboratory. Each section has flanges turned outward, allowing the individual sections to be bolted together. A circular configuration would not easily permit the use of flanges. They would have to be made separately and then brazed on. The square design resulted in a strong, solid structure.

The dimensions of the outer conductor were chosen to provide enough separation from the inner conductor to prevent arcing between the two. The maximum possible voltage on the transmission line is 50 KV, thus a separation distance of two inches was chosen to provide a reasonable margin of safety. The pulse width is directly dependent on the length of the transmission line. I was designing for maximum pulse width, so the line length was based on the physical dimensions of the room where it would be situated, the Quantum Electronics Laboratory. The resulting outer dimensions of the square coaxial transmission line are, eight inches wide by eight inches in height by six meters in length.

The center conductor is held in position by the use of spacers constructed from 1/2 inch acrylic sheets. A total of six spacers are used in the transmission line. They are separated by approximately one meter. In addition to the center hole for the copper pipe, a large hole was cut in each corner to remove extraneous material and to further

reduce the already low attenuation effect that the presence of the spacers create. The spacers are held in position by screws.

The spark gap is used as a high voltage switch. Two spheres one inch in diameter were machined out of bronze. Extending smoothly from each sphere is a 1/4 inch diameter shaft, two to three inches in length. One shaft, which is threaded at the end, is attached to the outer conductor of the transmission line, i.e. the ground plane, and the other is in series with the cell holder which acts as the termination resistor. The cell holder will be considered in the next chapter. The spheres are aligned to form the spark gap. The threaded shaft allows the distance between the spheres to be varied.

Characteristic Impedance

The characteristic impedance of a square coaxial line can easily be determined by graphical field mapping techniques. Figure 2.2 shows a sketch of the field lines and the equipotential lines for a cross-section of the square coaxial line. For a two conductor system, the capacitance per unit length is:

$$C = \frac{Q}{\phi_2 - \phi_1}$$

where: Q = the charge induced on a conductor

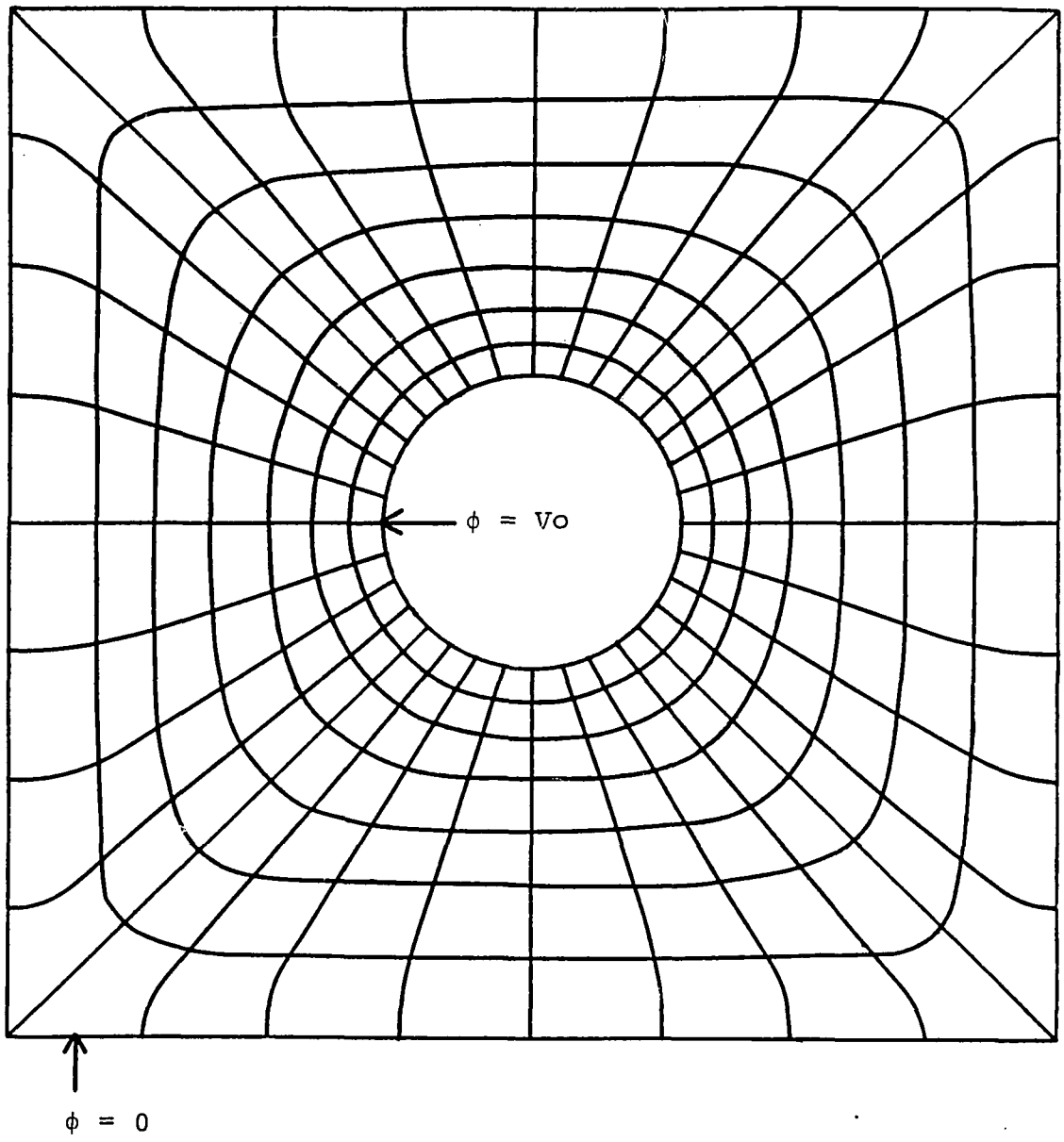

Figure 2.2. Transmission line cross-section, including E-field and equipotential lines.

$\phi_2-\phi_1$ = the potential difference between the conductors

By Gauss's law, the charge on a conductor is equal to the flux ending there. Also, the potential difference between the conductors is equal to the number of potential divisions multiplied by the potential difference per division. Therefore:

$$C = \frac{N_f \Delta\psi}{N_p \Delta\phi} \qquad (2.1)$$

where: N_f = the number of flux tubes

$\Delta\psi$ = the flux per tube

N_p = the number of potential divisions

$\Delta\phi$ = the potential difference per division

Isolating one curvilinear rectangle we have:

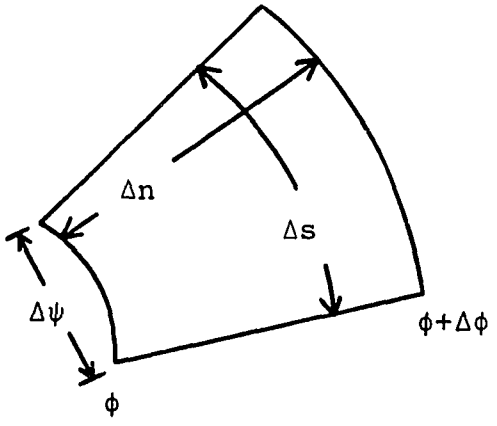

Figure 2.3. Isolated curvilinear rectangle.

where: Δn = the distance between two adjacent equipotentials

Δs = the distance between two adjacent field lines

Therefore, $\Delta\psi = D\Delta s = \varepsilon E\Delta s$ but $E = \frac{\Delta\phi}{\Delta n}$, thus $\Delta\psi = \varepsilon \frac{\Delta s}{\Delta n} \Delta\phi$

$\Delta s/\Delta n$ gives the side ratio. If in our sketch we form curvilinear squares, as was done in Figure 2.2, then $\Delta s/\Delta n = 1$. Substituting back into equation 2.1 we have:

$$C = \varepsilon \frac{N_f}{N_p}$$

From the sketch in Figure 2.2, we have $N_f = 32$ and $N_p = 7$. Therefore, $C = 8.854 \times 10^{-12} \times \frac{32}{7} = 40.48 \times 10^{-12}$ farads/meter.

The characteristic impedance is given by:

$$Z_o = \sqrt{\frac{R+j\omega L}{G+j\omega C}}$$

For a low-loss transmission line, $R << \omega L$, $G << \omega C$, and $v = 1/\sqrt{LC} = 2.998 \times 10^8$ m/s. Therefore:

$$Z_o = \sqrt{L/C} = \sqrt{\frac{1}{c^2 v^2}} \qquad (2.2)$$

Assuming the square coaxial line to be low-loss, the result is:

$$Z_o = 82.40 \text{ ohms}$$

This value can be compared to the result of a formula based on a truncated series found in the Electronic Engineering Handbook, 2nd Edition, by Fink and Christiansen. The characteristic impedance of a square coax is given as:

$$Z_o = 138 \log_{10}\rho + 6.48 - 2.34A - 0.48B - 0.12C$$

where:

$$A = \frac{1 + 0.405\ \rho^{-4}}{1 - 0.405\ \rho^{-4}}$$

$$B = \frac{1 + 0.163\ \rho^{-8}}{1 - 0.163\ \rho^{-8}}$$

$$C = \frac{1 + 0.067\ \rho^{-12}}{1 - 0.067\ \rho^{-12}}$$

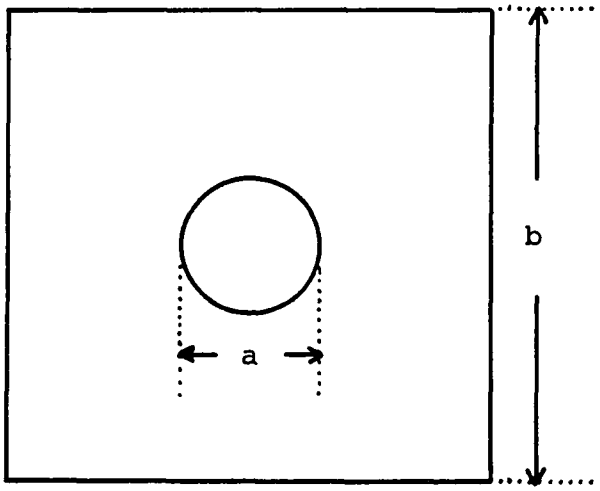

$$\rho = \frac{b}{a} = \frac{8}{2.25} = 3.556$$

Figure 2.4. Transmission line dimensions.

A = 1.005, B ≅ 1.000 and C ≅ 1.000; therefore, this formula results in Z_o = 79.554 ≅ 80 ohms, which closely matches the value found by graphical field mapping. The capacitance, based on this value of characteristic impedance, from equation 2.2 is:

$$C = 41.93 \times 10^{-12} \text{ farads/meter}$$

Pulse System Operation

Using the above results, we can now describe how the pulse system operates. The pulse system ideally produces a pulse train with a pulse duration of 40 nanoseconds, an amplitude of 25 KV and a somewhat variable pulse repetition frequency (PRF). The circuit can be viewed in two parts, a charging circuit and a discharging circuit. The charging circuit consists of the power supply, R_1 and the transmission line acting as a charging capacitor. The discharging circuit consists of the transmission line delivering energy to the load and then shorting to ground through the conducting spark gap.

Resistor R_1, through which the line is charged (see Figure 2.5), has a much higher value than the characteristic impedance, therefore, the 50 KV power supply is effectively isolated from the line during the brief discharge time. If the spark gap distance is large enough, the distributed capacitance of the line will be charged to 50 KV for as long as the power is applied. The distance of the spark gap is

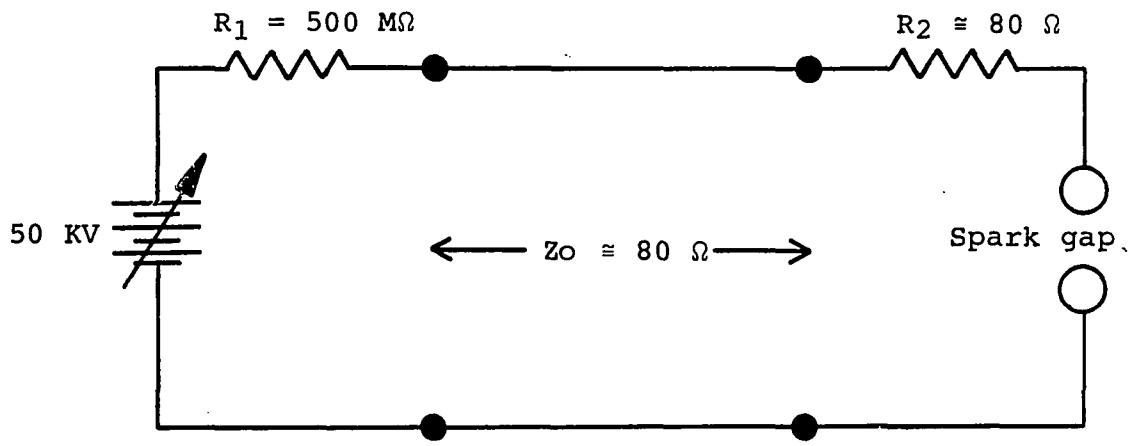

Figure 2.5. Abbreviated pulse system circuit.

adjusted so that a potential difference of approximately 50 KV appears between the spheres, causing the air within the spark gap to be ionized; the resulting plasma conducts, thus discharging the line. When the plasma starts to conduct, current starts to flow through R_2. The line may effectively be regarded as a battery with an internal impedance of 80 ohms during the discharge time. Assuming for the moment that the line is terminated exactly in its characteristic impedance, the voltage across R_2 is one half the voltage to which the line was charged, i.e. 25 KV, because half of the available voltage is dropped across the 80 ohm internal impedance of the line. The distributed inductance and capacitance of the line are so proportioned that the discharge rate is practically constant.

At the instant that the plasma starts to conduct, the voltage at point A falls to 25 KV. This can be regarded as a traveling wave of -25 KV applied at point A to reduce the voltage there immediately from 50 KV to 25 KV. On reaching point B, the wave sees effectively an open circuit, as $R_1 >> R_2$. The wave is reflected without change in polarity and immediately reduces the voltage at point B from 25 KV to 0 V. As the wave travels back to point A, the remaining 25 KV across the line is cancelled out. On reaching point A, the wave has reduced the voltage across all sections to zero, the wave itself disappearing because

it is absorbed in a load which ideally matches the characteristic impedance of the line.

The pulse formed across R_2 by the discharge lasts for the time required for the traveling wave to move from the spark gap end to the open end and back. If it is assumed that the spacers do not attenuate the wave velocity, then the wave velocity equals the speed of light. Therefore:

$$\text{Pulse Duration} = \frac{(2)(6\text{m})}{3\text{x}10^8 \text{ m/s}} = 40 \text{ nanoseconds}$$

The pulse repetition frequency can be varied by changing the length of the spark gap. The shorter the spark gap distance the lower the potential difference necessary to breakdown the air between the spheres. This results in a higher PRF but a correspondingly lower pulse magnitude. Thus, there is a tradeoff between high pulse frequency and high pulse magnitude. Raising one will lower the other. This is due to the charging time constant of the system which will be discussed in a later chapter. In general, the spark gap distance was set to yield the highest pulse magnitude possible. This resulted in a PRF of 2 to 5 Hz.

CHAPTER 3

CELL HOLDER DESIGN

The purpose of the cell holder is to contain a volume of cell solution (in our case the L1210 mouse leukemia cell line) in a non-toxic environment, enabling the solution to be effectively exposed to the particular treatment desired. The geometry of the cell holder is dependent upon the type of treatment. For example, if the cell solution is to be exposed to some chemotherapeutic drug, then a test-tube or petri dish would be an adequate cell holder, but on the other hand, if the cell solution is to be exposed to electromagnetic fields, then the cell holder must be of a more elaborate design. The intention of this work was to expose the cancerous cells to the maximum, uniform electric field possible, using the equipment discussed in the last chapter.

Parallel-Plate Cell Holder

The cell holder consists of two metal, circular plates separated by a doughnut shaped teflon disk. A hole bored into the periphery of the disk provides access to the resulting cavity. This parallel plate configuration was used successfully by Dr. R. C. Jones during his series of experiments. The dimensions of the holder are chosen to

result in an impedance which matches, as closely as possible, the characteristic impedance of the transmission line. Thus, the transmission line is terminated in the cell holder.

Instead of machining a new holder, to save expenses, the holders used by Dr. R. C. Jones were modified to function with the new pulse system. The modifications involved changing the geometry of the teflon disk and altering the manner in which the holder is connected to the transmission line. The transmission line used by Dr. R. C. Jones had a lower characteristic impedance than that used in the present system; therefore, the disk geometry was altered to increase the overall impedance of the cell holder. The impedance of the holder in its present form, filled with cell solution, was determined by measuring with a Hewlett Packard, Model 4815A, RF Vector Impedance meter. This instrument measures over a frequency range of 0.5 MHz to 108 MHz. The results of these measurements are shown in Table 3.1. The probe used to take these measurements was of a coaxial geometry, with the center conductor extended. The distance between this center conductor and the outer conductor was not great enough to allow direct measurements between the two plates of the cell holder, so that clips had to be attached to the cell holder (see Figure 3.1). The measurements were taken between these two attached clips,

Table 3.1. Impedance measurements of the filled cell holder, used by Dr. R. C. Jones

FREQUENCY (MHz)	MAGNITUDE (OHMS)	PHASE (DEG)	IMPEDANCE
1	19.0	-2	18.99-j0.66
2	18.0	0	18.00+j0.00
4	18.0	0	18.00+j0.00
6	18.0	+1	18.00+j0.31
8	18.0	+2	17.99+j0.63
10	17.5	+4	17.46+j1.22
12	17.5	+4	17.46+j1.22
14	18.0	+5	17.93+j1.57
16	17.5	+6	17.40+j1.83
18	18.5	+6	18.40+j1.93
20	17.0	+8	16.83+j2.37
22	17.0	+8	16.83+j2.37
24	17.5	+9	17.28+j2.74
26	17.5	+10	17.23+j3.04
28	17.5	+11	17.18+j3.34
30	18.0	+12	17.61+j3.74
50	18.0	+21	16.80+j6.45
70	19.5	+31	16.71+j10.0
100	22.0	+43	16.09+j15.0

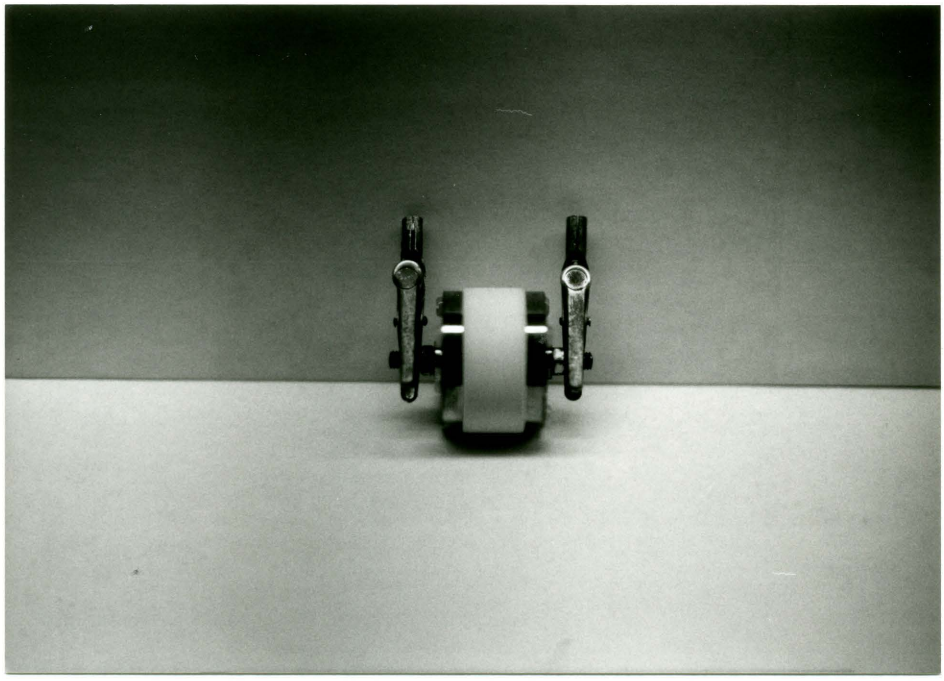

Figure 3.1. Cell holder with attached measurement clips.

and these clips probably account for the inductive effects seen in the measurements in Table 3.1.

It will be shown in a later chapter that for the resulting DC pulses most of the power is located at frequencies below 25 MHz. For this range of frequencies, and neglecting for the moment the imaginary components, the cell holder in its present form has an impedance of approximately 18 ohms. Using this value for impedance, we can determine the conductivity of the cell solution with the following relation:

$$Z = \frac{d}{\sigma A}$$

where: Z = the impedance of the cell holder

d = the distance between the parallel plates

A = the area of one plate = πr^2

σ = the conductivity of the material between the plates

r = the radius of the metal plate

The cell holder has a plate radius of 1.075 cm, and the distance between the plates is 0.7 cm. Rearranging the above relation, we have,

$$\sigma = \frac{d}{ZA} = \frac{0.7}{18\pi(1.075)^2} = 10.71 \text{ mmhos/cm}$$

The only variable which can be altered to yield a holder of 80 ohms, are those pertaining to the doughnut shaped teflon disk, i.e., the thickness or plate separation, d, and the radius of the inner cavity, r. Altering the conductivity of the cell solution would adversely affect the cells. Constraining the values for impedance and conductivity results in,

$$\frac{d}{r^2} = Z \sigma \pi = 2.692 \qquad (3.1)$$

To adequately perform the biological experiments later on, the holder should have a fluid capacity of at least 3 ml. The capacity of the cell holder is given by:

$$\text{capacity} = \pi r^2 d$$

For a capacity of 3 ml,

$$r^2 d = 0.955 \qquad (3.2)$$

Combining equations 3.1 and 3.2 results in r = 0.772 cm and d = 1.604 cm. Using this plate separation of 1.604 cm and assuming a maximum voltage of 50 KV on the transmission line would result in an electric field strength within the cell holder of,

$$50 \text{ KV} \cdot \frac{80}{80+80} \cdot \frac{1}{1.604 \text{ cm}} = 15.59 \text{ KV/cm}$$

Keeping the radius the same but decreasing the distance between the plates to 1.5 cm yields an impedance of,

$$Z = \frac{1.5}{(10.71\text{x}10^{-3})\pi(0.772)^2} \cong 75 \text{ ohms}$$

This results in an electric field strength within the cell holder of,

$$50 \text{ KV} \cdot \frac{75}{80+75} \cdot \frac{1}{1.5 \text{ cm}} = 16.13 \text{ KV/cm}$$

With r = 0.772 cm and d = 1.5 cm, the cell holder capacity is 2.79 ml, a volume sufficient to perform the necessary experiments. Trying to increase the electric field strength by further reducing the plate separation would not yield a large enough fluid capacity. The final dimensions chosen for the teflon disk are given in Figure 3.2.

This new cell holder consists of two circular metal plates separated by the doughnut shaped teflon disk. These three sections are held together by eight nylon screws. Nylon screws are used to prevent conduction between the two plates. On the inside portion of each metal plate there is a circular groove cut, into which an o-ring fits. When the two metal plates and the separating disk are screwed together, these o-rings press up against the disk, forming a fluid tight seal. A hole was bored through the top of the disk, down into the resulting cavity. The hole is just

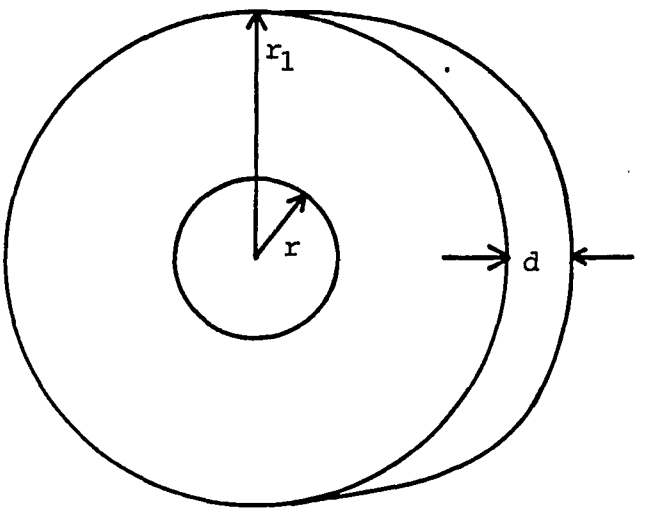

r = 0.77 cm, r_1 = 1.7 cm, d = 1.5 cm

Figure 3.2. Teflon disk dimensions.

large enough to allow a needle, which is attached to a syringe, to enter, thus allowing a way in which the cell solution can be put into or removed from the cell holder. All metal surfaces have been plated with gold, and o-rings made from viton have been used to ensure a non-toxic environment for the cells. The disk was machined out of teflon, as teflon is also non-toxic to the cells. A photograph of the holder with one plate removed, exposing the teflon disk in between, is shown in Figure 3.3.

As can be seen from Figure 3.3, extending outward from each metal plate is a half inch long bolt. One bolt is used to allow the cell holder to be connected to the center conductor of the transmission line, and the other bolt allows one of the spark gap spheres to be attached. The spark gap sphere is one inch in diameter, and extending smoothly from it is a two inch long, one quarter inch diameter shaft. The end of this shaft has internal threading allowing it to be screwed onto the bolt extending from the cell holder. The cell holder is thus in series with the center conductor of the transmission line and the spark gap. Figure 3.4 shows how these components are aligned.

The cell solution effectively sees a uniform electric field, because it is contained between two parallel plates. Due to the finite radius of the metal plates, there are some fringing effects present, but as shown in Table

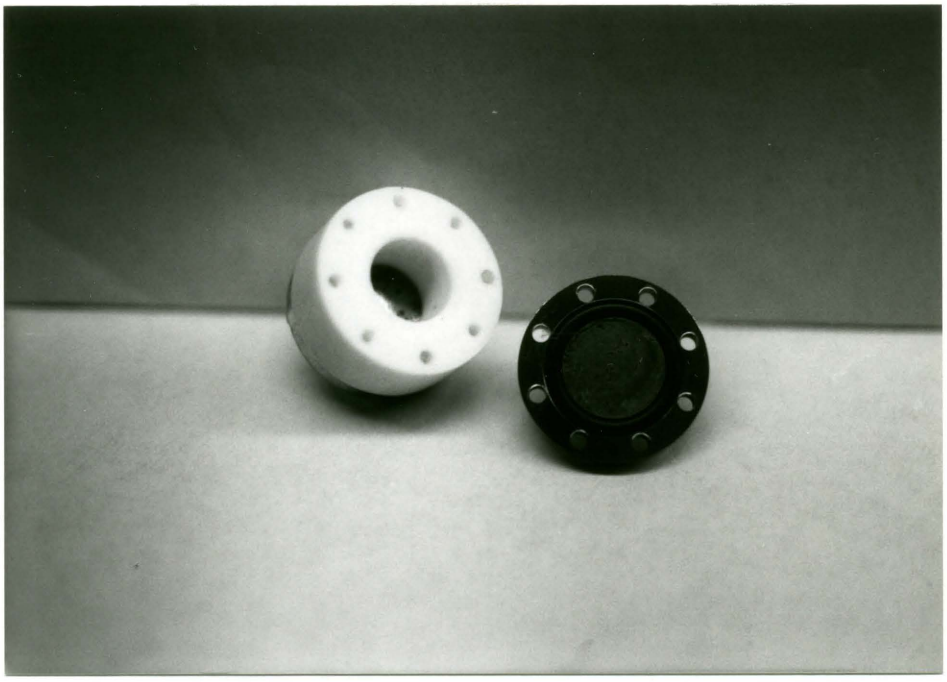

Figure 3.3. Cell holder with one plate removed, exposing the teflon disk.

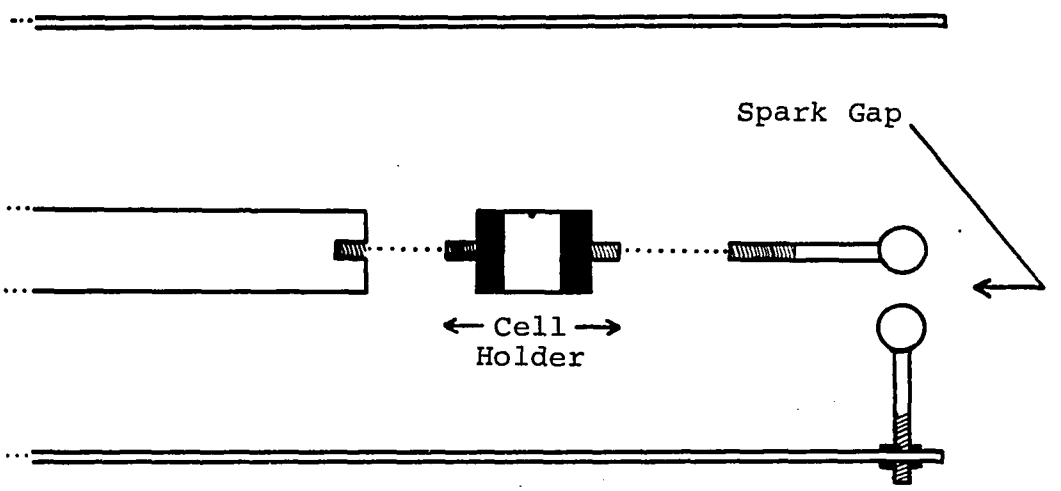

Figure 3.4. Transmission line with cell holder and spark gap.

3.1, they are essentially negligible. As this cell holder design meets all our requirements without any major problems, it was the choice for the biological experiments.

CHAPTER 4

PULSE SYSTEM ANALYSIS

Pulse System Charging

While the transmission line is charging, only a weak current is flowing as it essentially acts as a capacitor. The distributed shunt capacitance of the transmission line was found, in Chapter One, to be $C = 41.93 \times 10^{-12}$ farads/meter. The transmission line being six meters long, results in a total capacitance of:

$$C = 41.93 \times 10^{-12} \text{ farads/meter} \times 6 \text{ meters}$$
$$= 251.58 \times 10^{-12} \text{ farads}$$

When charging, the pulse system can be represented by the circuit shown in Figure 4.1.

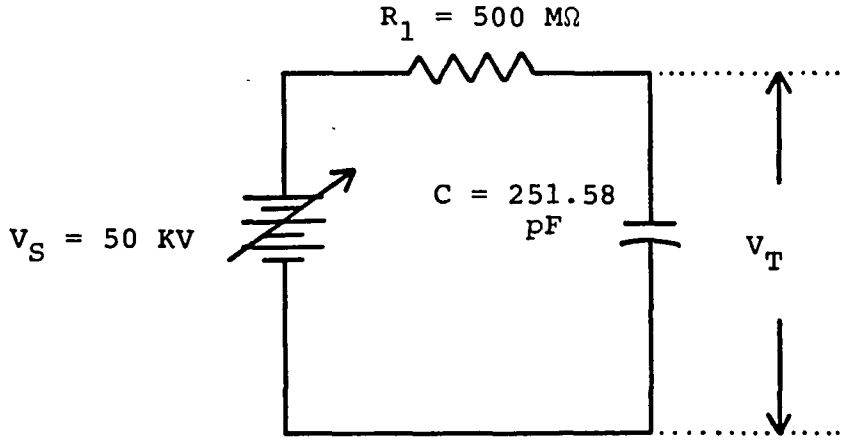

Figure 4.1. Pulse system charging circuit.

The time constant for the above circuit is:

$$\tau = RC = (500 \times 10^{6})(251.58 \times 10^{-12}) = 0.126 \text{ seconds}$$

The transmission line voltage, V_T, can therefore be expressed at any time by:

$$V_T = V_S(1 - e^{-t/\tau}) \qquad (4.1)$$

This relationship is useful in determining the actual voltage on the transmission line during an experiment, based on the measured number of pulses per second.

The spark gap distance varies slightly from one experiment to the next, causing the pulse repetition frequency (PRF) to vary. Thus, the pulse magnitude varies from one experiment to the next, depending upon the resultant PRF. Equation 4.1 can be rearranged to show the relationship between the pulse magnitude and the PRF.

$$\text{Maximum Pulse Magnitude} = \frac{V_T}{2}$$

$$= 25 \text{ KV } [1 - \exp(-1/0.126 \text{ PRF})] \qquad (4.2)$$

The maximum pulse magnitude is $V_T/2$ due to the following reason. Assuming, for the moment, that the transmission line is terminated exactly in its characteristic impedance; the moment the spark gap starts to conduct (i.e. the beginning of the pulse), the voltage across the cell holder (termination resistor) is one half the voltage

to which the transmission line was charged, because half the available voltage is dropped across the internal impedance of the line. Thus, the maximum pulse magnitude, i.e. voltage across the cell holder, is one-half the maximum transmission line voltage, V_T. Any mismatch in the termination will further reduce the maximum pulse magnitude.

The PRF obtained during the experiments ranged from 2 Hz to 5 Hz. Equation 4.2 can be put in graphical form, allowing an easy determination of pulse magnitude as a function of PRF.

Figure 4.2 graphically illustrates the inverse functional relationship between the pulse magnitude and the PRF. The higher the PRF, the lower the resulting pulse magnitude. It was important to keep the PRF as low as possible to maximize the pulse magnitude, thereby obtaining a high electric field within the cell holder.

Figure 4.3 shows the transmission line voltage, V_T, and the pulse magnitude occurring during a one second duration, where the PRF is, for example, 4 Hz. Note that the dimensions of the pulse are exaggerated to provide resolution.

For a PRF of 4 Hz, the transmission line is discharging every 0.25 seconds. At 0.25 seconds, the transmission line has charged to a voltage of 43.12 KV, according to equation 4.1. At this moment the air within the spark gap ionizes, and the resulting plasma starts to conduct. As the

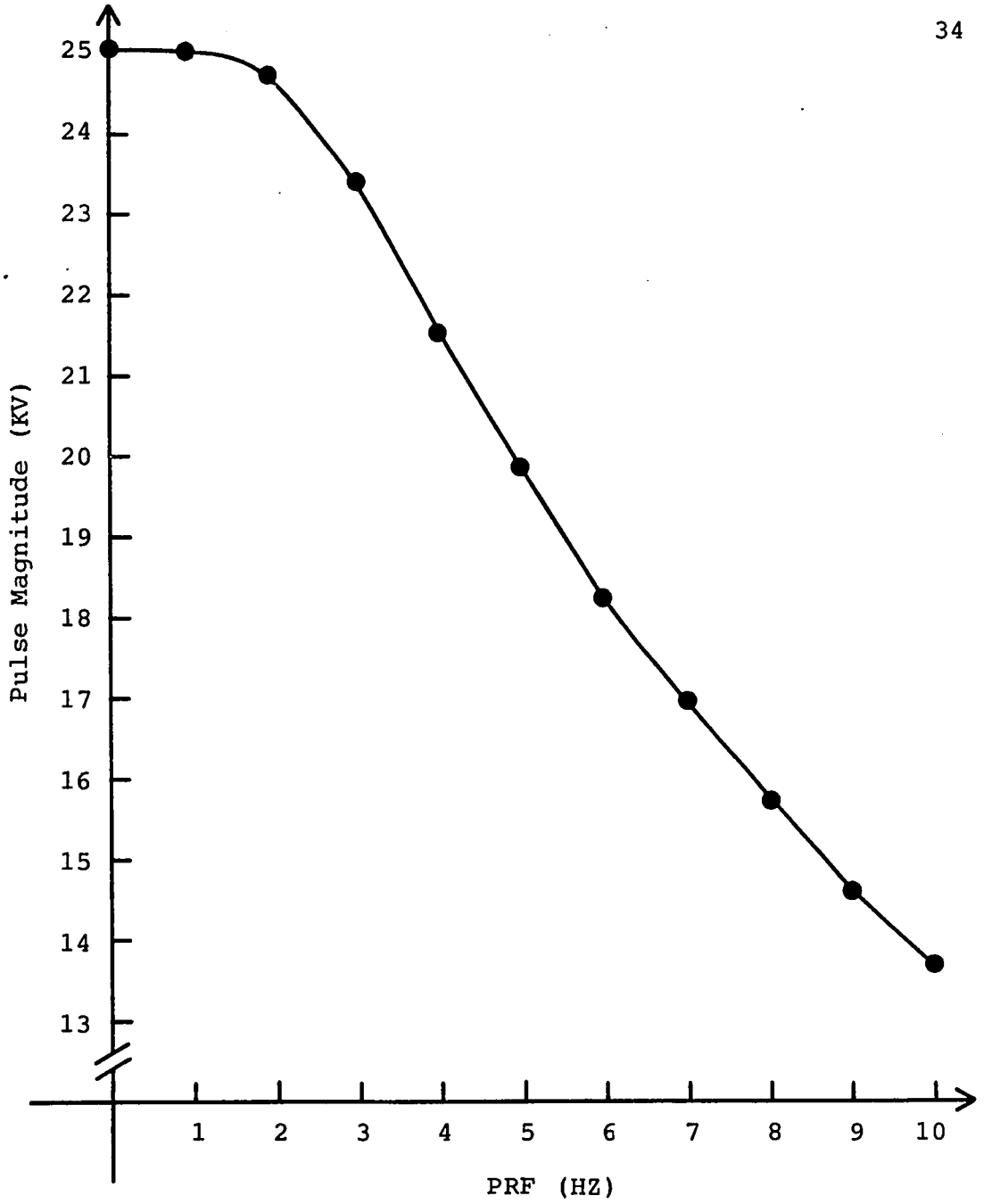

Figure 4.2. Pulse magnitude as a function of the pulse repetition frequency for the matched termination.

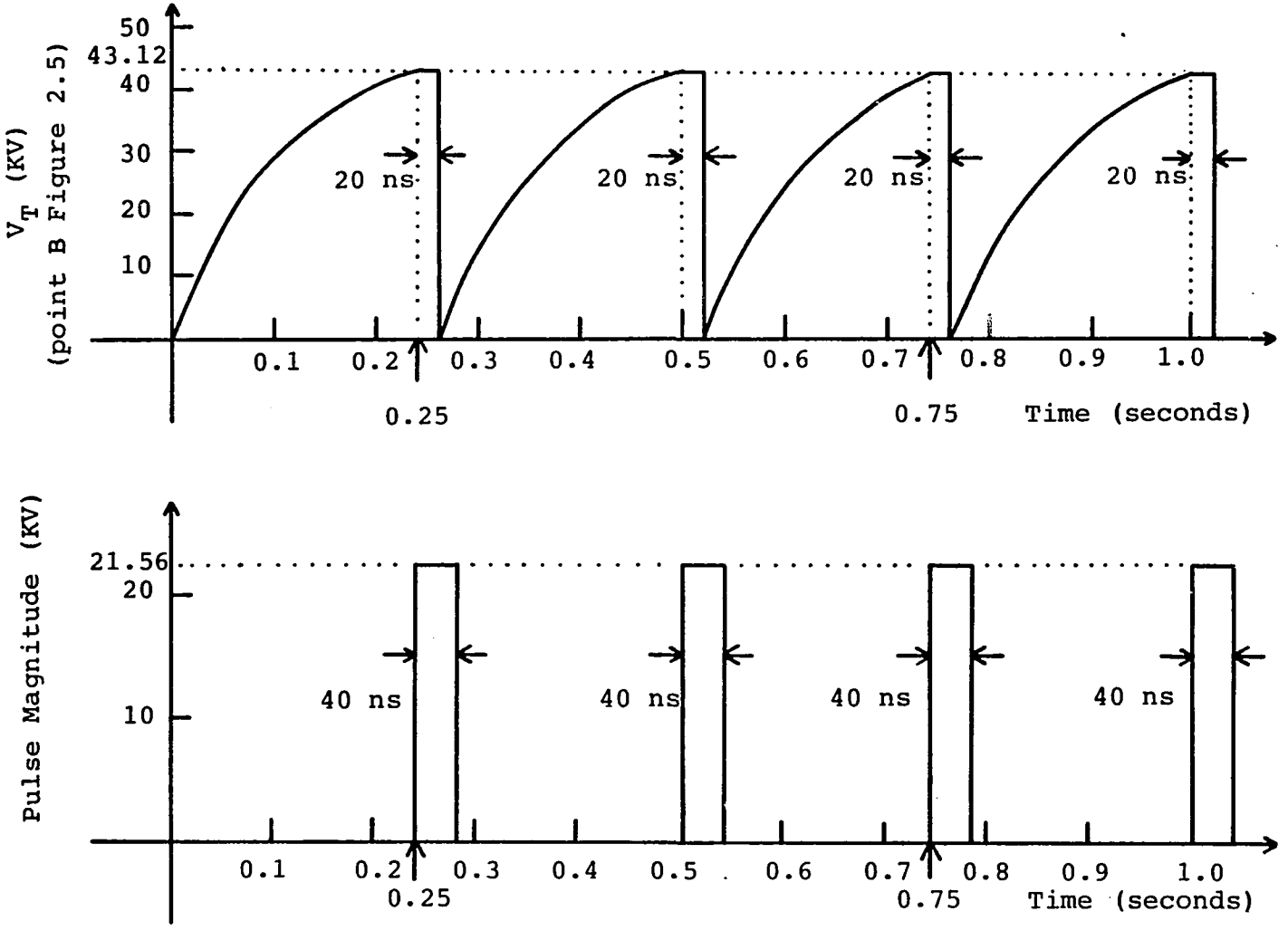

Figure 4.3. Transmission line voltage, V_T, and pulse magnitude as a function of time.

spark gap starts to conduct, the voltage across the cell holder, point A in Figure 2.5, rises nearly instantaneously from 0 V to 21.56 KV. This is the initiation of the pulse. See Figure 2.5.

When the spark gap conducts, we can consider a traveling wave of -21.56 KV to be applied at point A, reducing the voltage there immediately from 43.12 KV to 21.56 KV. As the transmission line is six meters long, it takes the traveling wave 6 meters/3 x 10^8 m/s = 20 ns to reach point B, reducing the voltage along the line to 21.56 KV as it progresses. Thus, the voltage at point B is maintained at 43.12 KV for 20 ns, i.e. the time it takes for the wave to reach that point. When the wave reaches point B it effectively sees an open circuit, as $R_1 >> R_2$. The wave is therefore reflected without change in polarity and immediately reduces the voltage at point B from 21.56 KV to 0 V. It then takes the reflected wave another 20 ns to progress from point B back to point A, reducing the voltage along the line from 21.56 KV to 0 volts. Hence, the voltage across the cell holder, i.e. the pulse, is maintained for a total of 40 ns. The pulse duration is clearly independent of the particular PRF, as it is constrained only by the length of the transmission line. The only pulse parameter which varies from one experiment to the next is the magnitude, which is dependent on the PRF.

Transmission Line Mismatch Analysis

In Chapter Three, the necessity of constructing the parallel-plate cell holder such that its overall impedance is less than 80 ohms was discussed. This section will discuss the change in the pulse resulting from this termination mismatch.

The mismatch between the characteristic impedance of the transmission line, Zo, and the impedance of the cell holder (i.e. the termination impedance, Z_ℓ), creates a discontinuity. By Kirchhoff's laws, the total voltage and current must be continuous across this discontinuity. The total voltage on the line, at the point of discontinuity, is equal to the sum of the voltage in the positive traveling wave and the voltage in the negative traveling wave. Thus,

$$V = V+ + V- \tag{4.3}$$

where: V = the total voltage at the point of discontinuity, i.e. across the junction

V+ = the voltage of the positive traveling wave at the discontinuity

V- = the voltage of the negative traveling wave at the discontinuity

Likewise, the sum of the current in the positive and negative traveling waves of the line must be equal to the current flowing into the junction, yielding

$$I = I+ + I- \tag{4.4}$$

The ratio of voltage to current for the wave traveling in the positive direction is:

$$\frac{V+}{I+} = Zo \tag{4.5}$$

For the reflected wave traveling in the opposite direction, the ratio of voltage to current is:

$$\frac{V-}{I-} = -Zo \tag{4.6}$$

With the line terminated in an impedance Z , the ratio of V to I at this point will be equal to Z , giving

$$Z\ell = \frac{V}{I} = \frac{V+ + V-}{I+ + I-} = Zo\,\frac{I+ - I-}{I+ + I-} \tag{4.7}$$

Substituting equation 4.7 into equation 4.4 yields

$$\frac{V}{Z\ell} = I+ + I-$$

The values for I+ and I- from equations 4.5 and 4.6 respectively can now be inserted to obtain

$$\frac{V}{Z\ell} = \frac{V+}{Zo} - \frac{V-}{Zo}$$

Inserting the value for V from equation 4.3 and then rearranging results in

$$\Gamma = \frac{V-}{V+} = \frac{Z\ell - Zo}{Z\ell + Zo}$$

where: Γ = the reflection coefficient, defined as the voltage ratio of the reflected wave to the forward wave.

The transmission line actually has two discontinuities, occurring at points A and B on Figure 4.4. A reflection coefficient can be calculated for each discontinuity. For point A, the load, we have

$$\Gamma\ell = \frac{Z\ell - Zo}{Z\ell + Zo} = \frac{63 - 80}{63 + 80} = -0.119$$

Note that a value of 63 ohms has been used for the load impedance. In the next chapter it will be shown that the measured value of impedance for the cell holder is approximately 63 ohms, and it is this value which will be used for the following mismatch analysis.

For point B, the source, we have

$$\Gamma s = \frac{Zs - Zo}{Zs + Zo} = \frac{500 \times 10^6 - 80}{500 \times 10^6 + 80} \cong 1.000$$

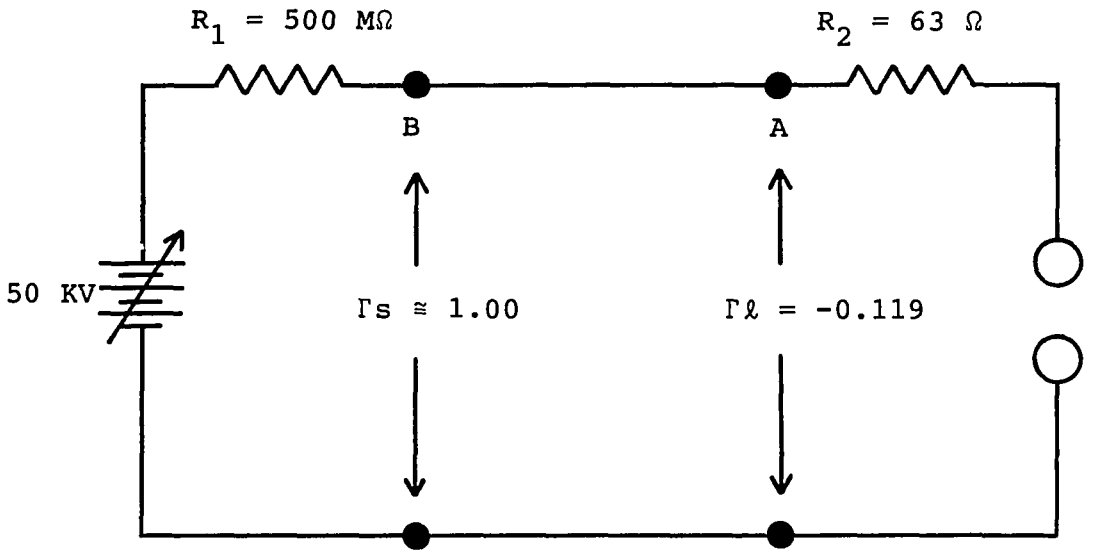

Figure 4.4. Mismatched pulse system circuit with discontinuities at points A and B.

Using these reflection coefficients, we can now determine how the termination mismatch affects the pulse. This will be accomplished by using a numerical presentation of the method of traveling waves. This method allows study of the time variation of the voltage at each point of the transmission line when reflection coefficients are different from zero.

For this analysis, let us extend our prior example (where the PRF is 4 Hz, and the maximum voltage on the line is 43.12 KV); now, we will determine the effects when R2 = 63 ohms.

A wave traveling from point A to point B takes a total time of 6 m/3 x 10^8 m/s = 20 ns. This will be referred to as time t, to distinguish it from the time constant τ. For the moment let us normalize the initial pulse amplitude to one. The actual voltages will be determined later.

At the moment of discharge, a traveling wave of unity amplitude is initiated at point A, see Figure 4.4. At time t, the wave reaches point B. At this instant, the incident wave is reflected with Γs = 1.00. Thus, a wave of unity amplitude is reflected back towards point A. The change in amplitude at point B, for time t, is now 1 + Γs or 2. When the reflected wave of unity amplitude reaches point A, at time 2t, it is reflected with $\Gamma \ell$ = -0.119. A wave of amplitude (1)(-0.119) or -0.119 is reflected back towards

point B. The change in amplitude, at point A, for time 2t, is therefore, $\Gamma s\ (1 + \Gamma \ell)$ or $(1)(1 - 0.119) = 0.881$. When the reflected wave of amplitude -0.119 reaches point B, at time 3t, it is reflected with $\Gamma s = 1.00$. Thus, a wave of amplitude $(1)(-0.119) = -0.119$ is reflected back towards point A. The change in amplitude at point B, for time 3t, is now $\Gamma s \Gamma \ell (1 + \Gamma s)$ or $(1)(-0.119)(1 + 1) = -0.238$. The reflected wave of amplitude -0.119 reaches point A, at time 4t, and it is reflected with $\Gamma \ell = -0.119$. The wave reflected back towards point B has an amplitude of $(-0.119) \cdot (-0.119) = 1.42 \times 10^{-2}$. The change in amplitude, at point A, for time 4t, is $\Gamma \ell \Gamma s^2\ (1 + \Gamma \ell)$ or $(-0.119)(1)^2 \cdot (1 - 0.119) = -0.105$. The reflected wave of amplitude 1.42×10^{-2} reaches point B, at time 5t. It is reflected with $\Gamma s = 1.00$. A wave of amplitude $(1.00)(1.42 \times 10^{-2})$ is reflected back towards point A. The change in amplitude, at point B, for time 5t, is $\Gamma s^2 \Gamma \ell^2 (1 + \Gamma s)$ or $(1)(-0.119)^2 \cdot (1 + 1)$ or 2.83×10^{-2}. These calculations have been carried out through time 10t, and the results are presented to Table 4.1.

The values shown in the point A and point B columns represent only the change in voltage amplitude. To get the total voltage resulting from these changes, their values must be summed. For example, the total voltage at point A, for time 2t, is 1 + 0.881 or 1.88 and the total voltage, at point B, for time 5t, is $2 - 0.238 + 2.83 \times 10^{-2}$ or 1.79.

Table 4.1. Change in normalized voltage amplitude versus time for the pulse signal

TIME t = 20 ns	CHANGE IN NORMALIZED VOLTAGE AMP. (POINT A)	CHANGE IN NORMALIZED VOLTAGE AMP. (POINT B)
0	1.00	
t		2.00
2t	0.881	
3t		-0.238
4t	-0.105	
5t		2.83×10^{-2}
6t	1.25×10^{-2}	
7t		-3.38×10^{-3}
8t	-1.49×10^{-3}	
9t		4.01×10^{-4}
10t	1.77×10^{-4}	

But, these are only the normalized voltages. To find the actual values we need to know the actual voltage amplitude at t = 0. With the transmission line charged to 43.12 KV, the moment discharge occurs, the voltage at point A (the voltage drop across the cell holder) rises instantaneously (ideally) from 0 V to

$$43.12 \text{ KV} \cdot \frac{63}{63 + 80} = 19.00 \text{ KV}.$$

Thus, a wave of amplitude 19.00 KV - 43.12 KV = -24.12 KV is initiated, at point A, at time t = 0. To find the actual voltage changes, the normalized values in Table 4.1 are multiplied by the initial wave amplitude, -24.12 KV. These values are given in Table 4.2.

To find the actual voltage on the transmission line, these voltage changes are summed, and the result is added to 43.12 KV, the initial voltage on the line. These values are shown in Table 4.3, and the voltages at point A, which are the pulses of concern, are graphed in Figure 4.5.

The values in Table 4.3 suggest that the pulse signal may stabilize to some positive value, but it actually stabilizes to 0 V. Many more significant digits must be used in the above analysis for the values in Table 4.3 to show this. This can be proved, however, by noting that the column values, in Table 4.1, form a geometric series. At t = ∞ , it is possible to show that the two series, obtained

Table 4.2. Change in voltage amplitude versus time for the pulse signal.

TIME t = 20 ns	CHANGE IN VOLTAGE AMP. (POINT A)	CHANGE IN VOLTAGE AMP. (POINT B)
0	-24.12 KV	
t		-48.25 KV
2t	-21.25 KV	
3t		5.741 KV
4t	2.533 KV	
5t		-682.7 V
6t	-301.5 V	
7t		81.54 V
8t	35.94 V	
9t		-9.673 V
10t	-4.270 V	

Table 4.3. Voltage amplitude versus time for the pulse signal.

TIME t = 20 ns	VOLTAGE AMPLITUDE (POINT A)	VOLTAGE AMPLITUDE (POINT B)
0	19.0 KV	
t		-5.13 KV
2t	-2.25 KV	
3t		611.0 V
4t	283.0 V	
5t		-71.70 V
6t	-18.5 V	
7t		9.84 V
8t	17.44 V	
9t		0.167 V
10t	13.17 V	

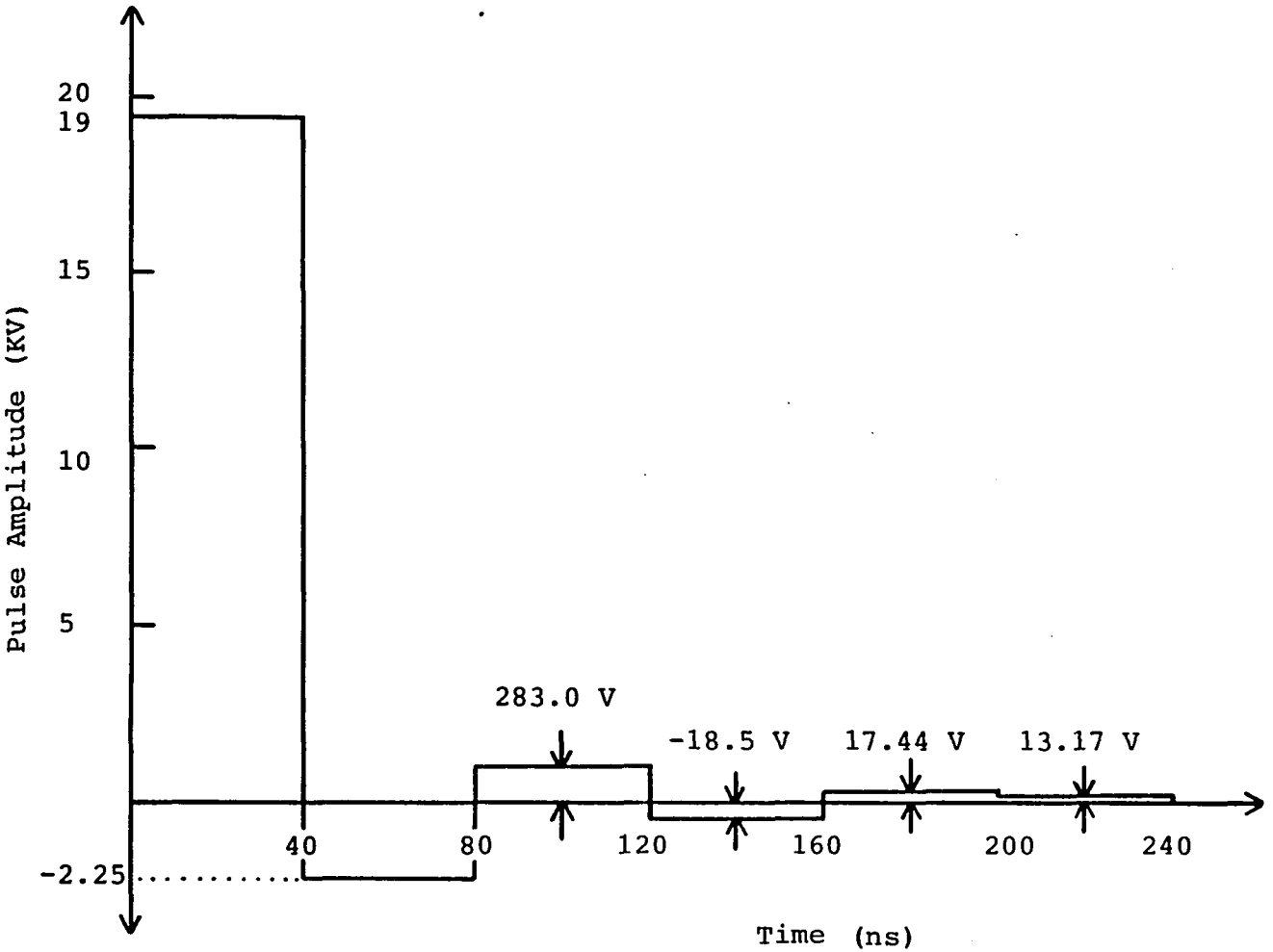

Figure 4.5. Pulse amplitude versus time for the mismatched termination.

by summing the terms in Table 4.1, converge to the same limit:

$$\frac{1 + \Gamma s}{1 + \Gamma s \Gamma \ell}$$

Thus, at $t = \infty$, the normalized voltage amplitude is,

$$\frac{1 + 1}{1 + (1)(-0.118881119)} = 1.7875$$

and the final voltage on the transmission line is:

$$43.12 \text{ KV} + (1.7875)(-24.123076 \text{ KV}) = 0.000010 \text{ V}$$

The maximum pulse amplitude due to the mismatched termination is only 2.56 KV below that of the matched termination pulse amplitude. The pulse amplitude has decreased to negligible proportions after approximately 120 ns. When compared to the time constant of $\tau = 0.126$ seconds, the reflections arising due to the mismatched termination have no effect on the pulse system charging, and thus have no effect on subsequent pulse formation.

Pulse-Frequency Spectrum

The first step in determining the major frequency components for the pulses produced by the equipment described in chapter two, is to derive a mathematical expression for this pulsed signal. The Fourier series is the

mathematical device used. It allows any repeating pulse to be represented by a series of sinusoidal components, where all frequencies are harmonically related. Therefore, a pulse may be analyzed as being composed of a DC component, a fundamental frequency, and an infinite number of harmonics. The amplitude and phase of each harmonic is dependent upon the shape and characteristics of the pulse.

For this analysis, let us first look at the spectrum of our actual pulse (due to the mismatched termination), and then compare it to a perfectly rectangular pulse.

The pulse signal is shown in Figure 4.5. It consists of six different sections. The amplitudes of each will be denoted A1 through A6. Thus, from Figure 4.5: for $0 < t \leq \tau$ (where $\tau = 40$ ns), A1 = 19 KV; for $\tau < t \leq 2\tau$, A2 = -2.25 KV; for $2\tau < t \leq 3\tau$, A3 = 283 V; for $3\tau < t \leq 4\tau$, A4 = -18.5 V; for $4\tau < t \leq 5\tau$, A5 = 17.44 V; and for $5\tau < t \leq 6\tau$, A6 = 13.17 V. For time $> 6\tau$ we will assume the pulse amplitude has decreased to 0 V (i.e. A7 = 0 V).

This signal can be represented by the following trigonometric series

$$f(t) = a_o + \sum_{n=1}^{\infty} [a_n \cos(n\omega_o t) + b_n \sin(n\omega_o t)] \qquad (4.8)$$

Euler's formulas allow one to determine the Fourier coefficients a_o, a_n, and b_n.

$$a_o = \frac{1}{T} \int_{t1}^{t2} f(t)\ dt$$

$$a_n = \frac{2}{T} \int_{t1}^{t2} f(t)\ \cos(n\omega_o t)\ dt$$

$$b_n = \frac{2}{T} \int_{t1}^{t2} f(t)\ \sin(n\omega_o t)\ dt$$

Because the pulse has six different components, the coefficients will need to be determined for each component, and then summed to yield the final coefficient value. To illustrate this, equation 4.8 can be rewritten as

$$f(t) = \sum_{m=1}^{6} a_{om} + \sum_{n=1}^{\infty} \left[\sum_{m=1}^{6} a_{nm}\cos(n\omega_o t) + \sum_{m=1}^{6} b_{nm}\sin(n\omega_o t) \right] \qquad (4.9)$$

The coefficients, a_{om}, are evaluated as follows:

$$a_{o1} = \frac{1}{T} \int_{0}^{\tau} A1\ dt = \frac{A1\tau}{T}$$

The others are determined in a similar fashion, yielding

$$a_{o2} = \frac{A2\tau}{T}$$

$$a_{o3} = \frac{A3\tau}{T}$$

$$a_{o4} = \frac{A4\tau}{T}$$

$$a_{o5} = \frac{A5\tau}{T}$$

$$a_{o6} = \frac{A6\tau}{T}$$

This may be written in closed form as:

$$a_o = \frac{\tau}{T} \sum_{m=1}^{6} A_m \tag{4.10}$$

The coefficients a_{nm} are evaluated as follows:

$$a_{n1} = \frac{2}{T} \int_0^{\tau} A1 \cos(n\omega_o t)\, dt = \frac{2A1}{n\omega_o T} \sin(n\omega_o \tau)$$

likewise,

$$a_{n2} = \frac{2A2}{n\omega_o T} [\sin(n\omega_o 2\tau) - \sin(n\omega_o \tau)]$$

$$a_{n3} = \frac{2A3}{n\omega_o T} [\sin(n\omega_o 3\tau) - \sin(n\omega_o 2\tau)]$$

$$a_{n4} = \frac{2A4}{n\omega_o T} [\sin(n\omega_o 4\tau) - \sin(n\omega_o 3\tau)]$$

$$a_{n5} = \frac{2A5}{n\omega_o T} [\sin(n\omega_o 5\tau) - \sin(n\omega_o 4\tau)]$$

$$a_{n6} = \frac{2A6}{n\omega_o T} [\sin(n\omega_o 6\tau) - \sin(n\omega_o 5\tau)]$$

The closed form for a_n is

$$a_n = \frac{2\tau}{T} \sum_{m=1}^{6} m(A_m - A_{m+1}) \frac{\sin(n\omega_o m\tau)}{n\omega_o m\tau} \qquad (4.11)$$

The coefficients b_{nm} are evaluated as follows:

$$b_{n1} = \frac{2}{T} \int_0^{\tau} A1 \sin(n\omega_o t)\, dt = \frac{2A1}{n\omega_o T} [1 - \cos(n\omega_o \tau)]$$

In a similar fashion,

$$b_{n2} = \frac{2A2}{n\omega_o T} [\cos(n\omega_o \tau) - \cos(n\omega_o 2\tau)]$$

$$b_{n3} = \frac{2A3}{n\omega_o T} [\cos(n\omega_o 2\tau) - \cos(n\omega_o 3\tau)]$$

$$b_{n4} = \frac{2A4}{n\omega_o T} [\cos(n\omega_o 3\tau) - \cos(n\omega_o 4\tau)]$$

$$b_{n5} = \frac{2A5}{n\omega_o T} [\cos(n\omega_o 4\tau) - \cos(n\omega_o 5\tau)]$$

$$b_{n6} = \frac{2A6}{n\omega_o T} [\cos(n\omega_o 5\tau) - \cos(n\omega_o 6\tau)]$$

and in closed form,

$$b_n = \frac{2\tau}{T} \sum_{m=0}^{6} m(A_{m+1} - A_m) \frac{\cos(n\omega_o m\tau)}{n\omega_o m\tau} \qquad (4.12)$$

where $A0 \triangleq 0$

Equations 4.10, 4.11, and 4.12, when inserted into equation 4.8 give the final expression for the pulse signal f(t).

$$f(t) = \frac{\tau}{T} \sum_{m=1}^{6} A_m$$

$$+ \frac{2\tau}{T} \sum_{n=1}^{\infty} \{ [\sum_{m=1}^{6} m(A_m - A_{m+1}) \frac{\sin(n\omega_o m\tau)}{n\omega_o m\tau} \cos(n\omega_o t)]$$

$$+ [\sum_{m=0}^{6} m(A_{m+1} - A_m) \frac{\cos(n\omega_o m\tau)}{n\omega_o m\tau} \sin(n\omega_o t)] \} \qquad (4.13)$$

To determine the frequency components of this signal, it is necessary to calculate the magnitude of c_n, where

$$c_n = \pm\sqrt{a_n^2 + b_n^2}$$

From equations 4.11 and 4.12 we obtain

$$c_n = + \frac{2\tau}{T} \{ [\sum_{m=1}^{6} m(A_m - A_{m+1}) \frac{\sin(n\omega_o m\tau)}{n\omega_o m\tau}]^2 + [\sum_{m=0}^{6} m(A_{m+1} - A_m) \frac{\cos(n\omega_o m\tau)}{n\omega_o m\tau}]^2 \}^{1/2} \quad (4.14)$$

In keeping with past examples, this will be analyzed assuming a PRF = 4 Hz, thus T = 0.25 seconds and $\omega_o = 8\pi$. A plot of c_n versus frequency is shown in Figure 4.6. This graph shows the normalized voltage magnitude for a single pulse signal of an infinitely long pulsed train. The actual voltages are given in parenthesis. Spectral lines are found within the given envelope at intervals of 4 Hz.

To see how the mismatched termination affected the frequency spectrum let us perform a similar analysis on a perfectly rectangular pulse. This signal, f1(t) will have an amplitude of A, a pulse width τ, an interpulse period, T and an angular pulse repetition frequency of $\omega_o = 2\pi$ PRF. This signal is shown in Figure 4.7. Signal f1(t) is a periodic function of period T, thus it also can be represented by the Fourier series given in equation 4.8.

By positioning zero on the time axis in the center of one of the pulses, as shown in Figure 4.7, the coefficients, b_n, of the sine term are reduced to zero. This particular positioning of time zero makes the pulse symmetric about the vertical axis. Thus, f1(t) is an even

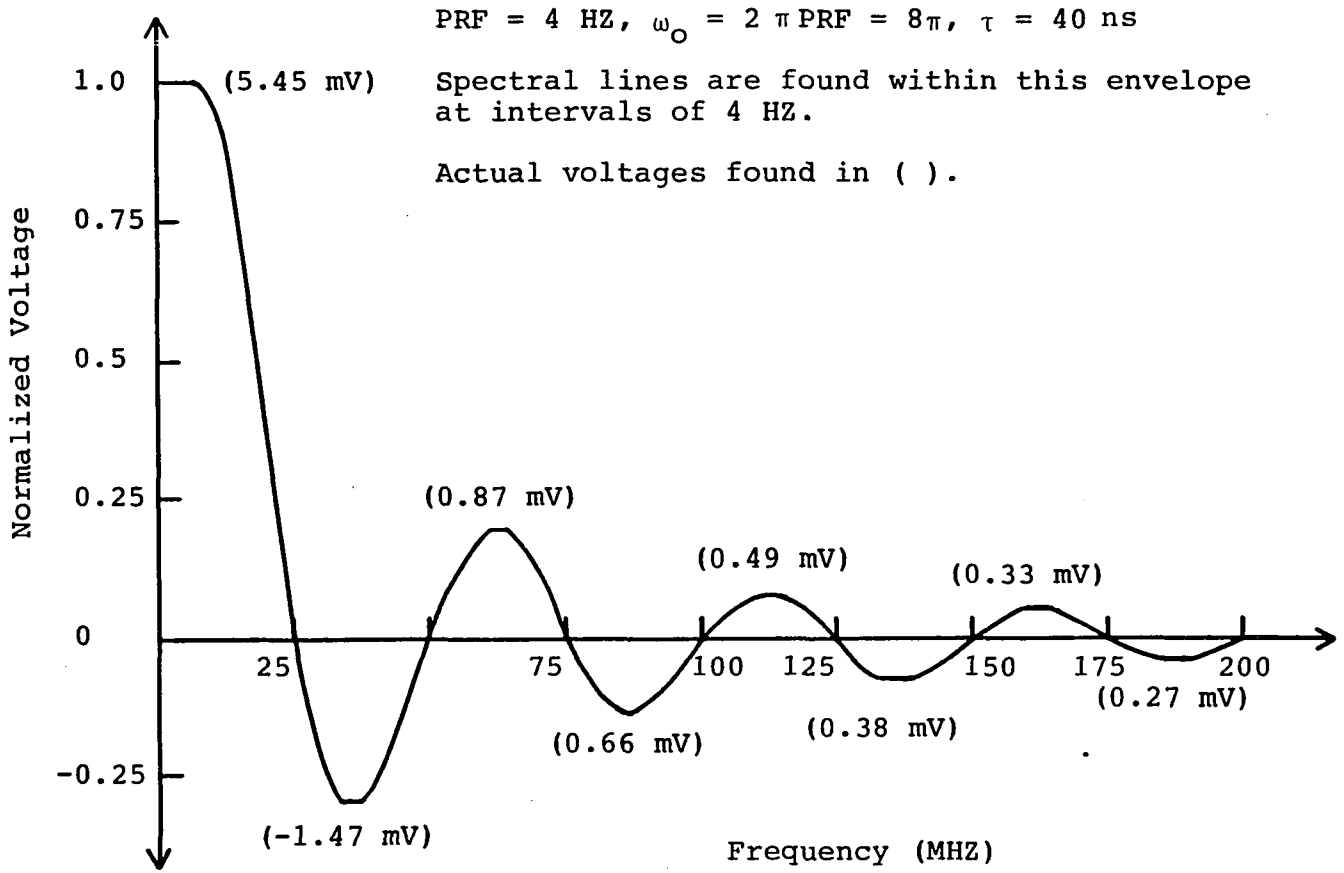

Figure 4.6. Spectral envelope for the mismatched termination (actual case).

$\omega_o = 8\pi$

$\tau = 40$ ns

$T = 0.25$ seconds

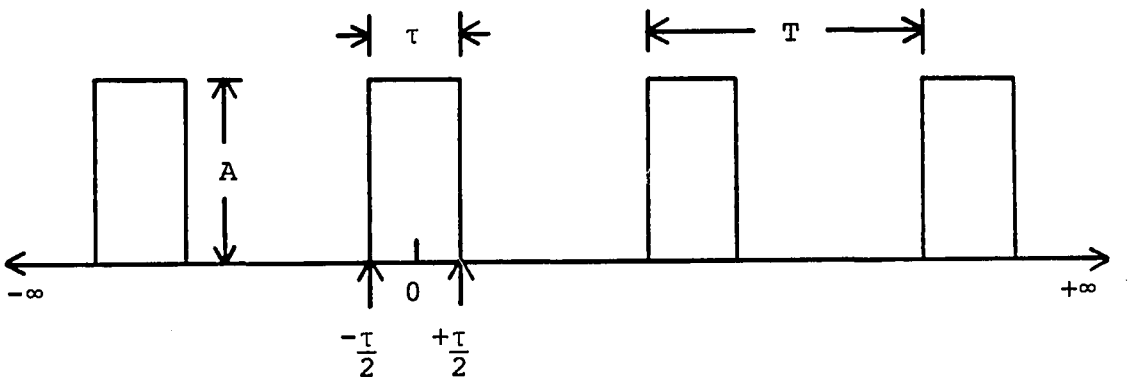

Figure 4.7. Ideal pulse train.

function. The sine term in the expression for b_n is an odd function. The product of an even function and an odd function is an odd function, and the integral of an odd function over a symmetric interval is zero. Therefore, all the b_n terms reduce to 0, and we are left with

$$f1(t) = a_o + \sum_{n=1}^{\infty} a_n \cos(n\omega_o t)$$

The coefficient, a_o, is evaluated as follows:

$$a_o = \frac{1}{T} \int_{-\tau/2}^{\tau/2} f1(t)\, dt$$

where, $f1(t) = A$ for $-\tau/2 \leq t \leq \tau/2$

0 for $\tau/2 < t < -\tau/2$

Therefore, $a_o = \frac{A\tau}{T}$

The coefficient, a_n, is evaluated as follows:

$$a_n = \frac{2}{T} \int_{-\tau/2}^{\tau/2} A \cos(n\omega_o t)\, dt = \frac{2A\tau}{T} \frac{\sin(n\omega_o \tau/2)}{n\omega_o \tau/2}$$

Therefore, $f1(t) = \frac{A\tau}{T} + \sum_{n=1}^{\infty} \frac{2A\tau}{T} \frac{\sin(n\omega_o \tau/2)}{n\omega_o \tau/2} \cos(n\omega_o t)$

Since $b_n = 0$, the coefficient, c_n, in this case is equal to a_n. Figure 4.8 shows a plot of normalized voltage

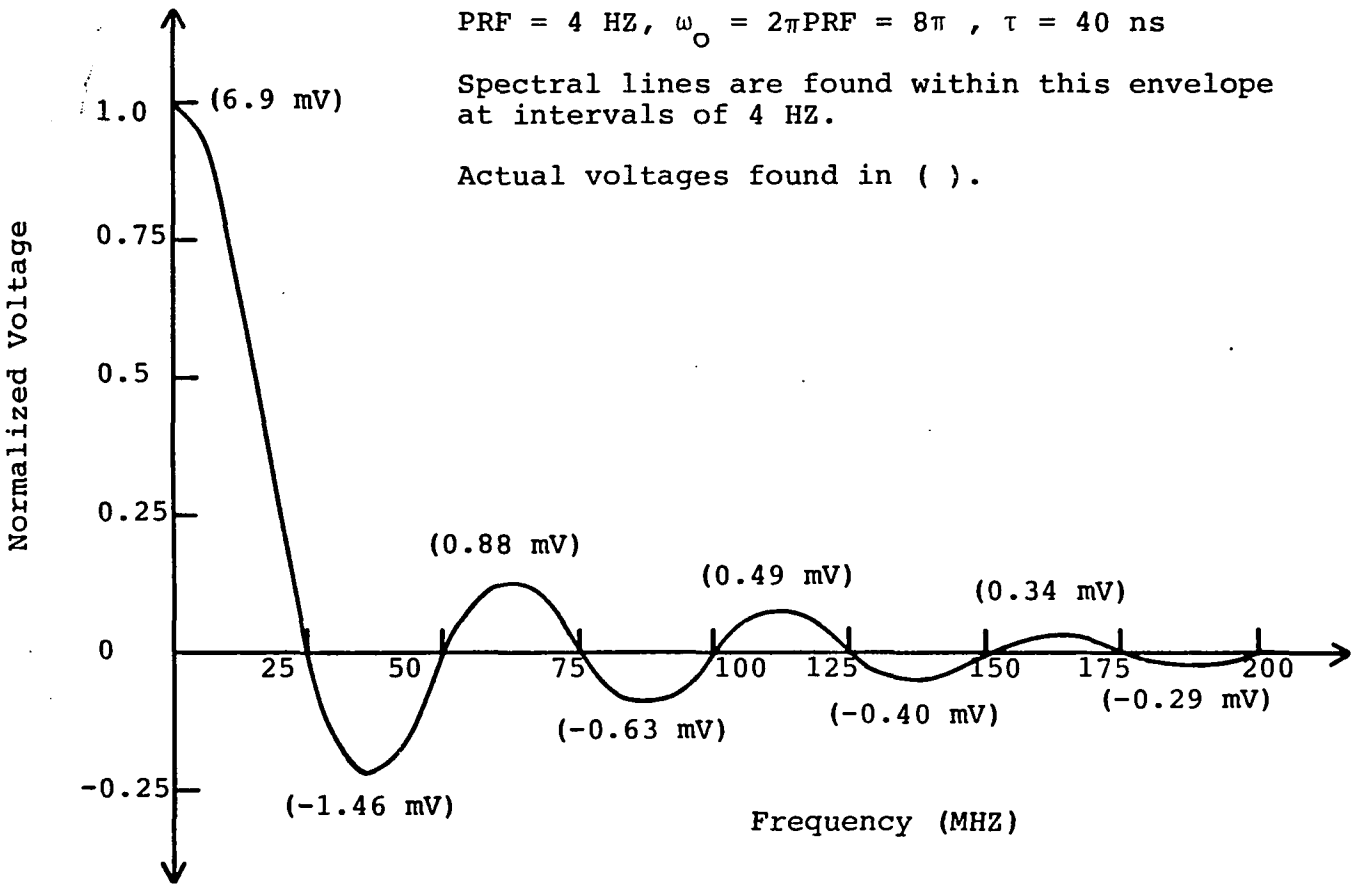

Figure 4.8. Spectral envelope for the matched termination (ideal case).

versus frequency for this ideal pulse. Once again, the actual voltage values are shown in parenthesis.

The spectral envelope for the ideal pulse, shown in Figure 4.8, is a true sin x/x shape. When this is compared to the actual spectral envelope, shown in Figure 4.6, several differences can be observed. In the actual spectral envelope, the secondary lobes have a higher amplitude relative to the initial lobe, and some of their peaks appear to be flattened. Also, some of the lobes do not appear to be symmetric, and the actual envelope voltage amplitudes are slightly lower than those of the ideal pulse spectral envelope.

Note that the above analysis assumes an infinite pulse train. For a finite pulse train, the spectral lines actually have a sin x/x shape, where the null-to-null width of the central lobe is equal to 2/NT where N = the number of pulses, and T = the interpulse period. As the exposure time, NT, increases toward infinity, the null-to-null width of the central lobe approaches zero and the sin x/x shape of the spectral line reduces to a single line. Figure 4.9 is a composite showing the envelope, spectral lines, null points, and spectral line null-to-null bandwidth of an ideal pulse signal. Note, for clarity only a few spectral lines are included.

Thus, the frequency spectrum envelope has a sin x/x shape (which is distorted, if the pulse is not perfectly

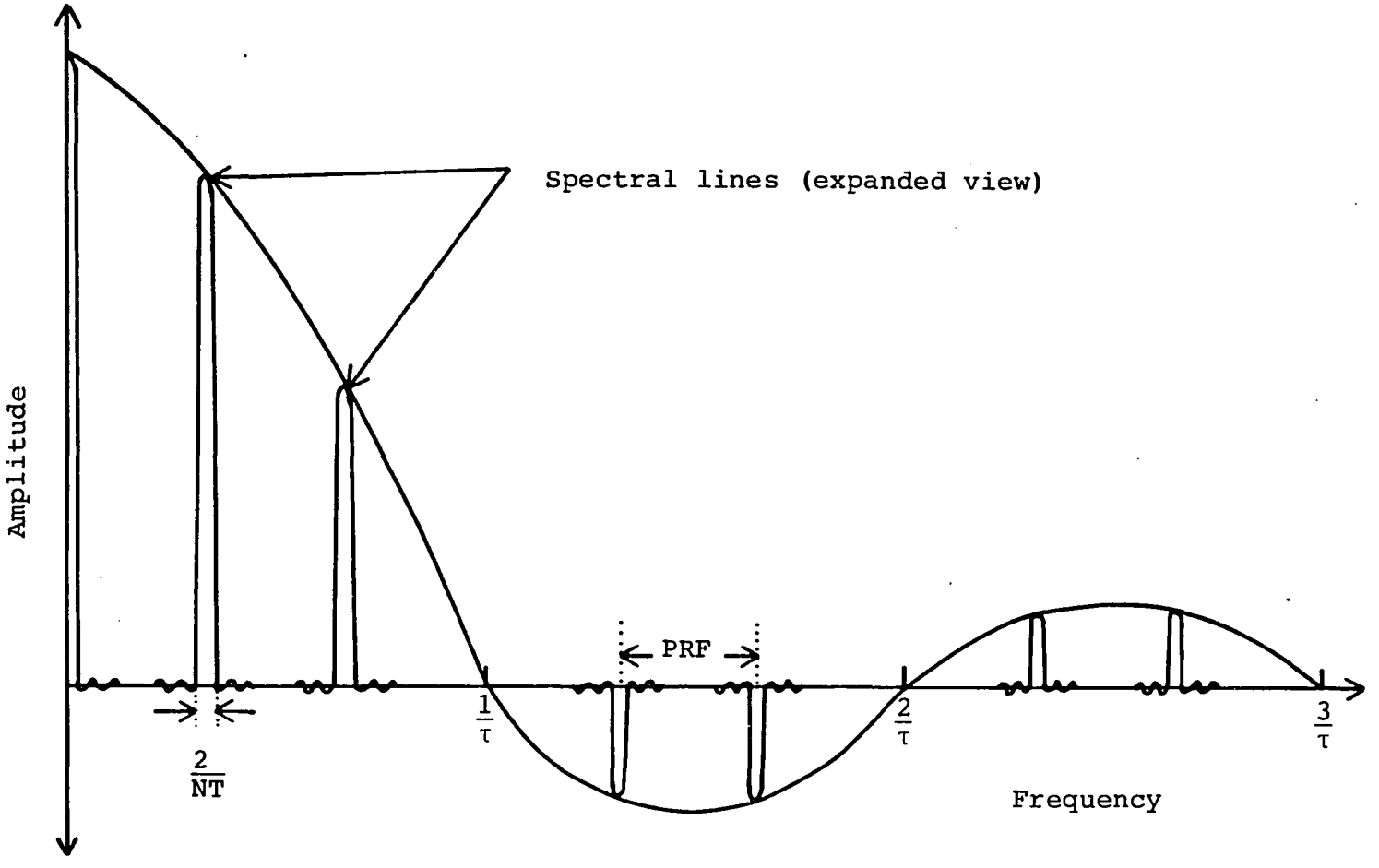

Figure 4.9. Fourier transform for a rectangular train of N DC pulses.

rectangular) with nulls found at integer multiples of $1/\tau$. The spectral lines, also having a sin x/x shape with a null-to-null width of 2/NT, occur at integer multiples of the PRF. For τ = 40 ns, PRF = 4 Hz, and an exposure time of NT = 1 hour = 3600 seconds, the envelope nulls occur at multiples of 25 MHz, and the spectral lines, having a null-to-null width of 5.56×10^{-4} Hz, occur at multiples of 4 Hz.

Signal Power and Energy

For the pulse signal shown in Figure 4.5, the maximum voltage amplitude is 19 KV. The maximum current through the load during discharge is simply I = V/R, where R is the load resistance. For a load resistance of 63 ohms, the maximum discharge current, I, equals 19 KV/63 ohms = 301.6 amps. The peak power is given by Ppeak = IV. For the above discharge current of 301.6 amps, the peak power of the individual pulse, is

$$\text{Ppeak} = IV = (301.6)(19 \times 10^3) = 5.73 \text{ MW}$$

The energy per pulse is equal to the peak power times the pulse width. The pulse signal in Figure 4.5 has six major components; the energy for each part must be found, and then summed to obtain the total energy per pulse signal.

$$\text{Energy/pulse signal} = \frac{40 \times 10^{-9}}{63} [(19\text{KV})^2 + (-2.25 \text{ KV})^2$$

$$+ (283\ V)^2 + (-18.5\ V)^2 + (17.44\ V)^2$$
$$+ (13.17\ V)^2]$$
$$= 0.232 \text{ joules}$$

For a exposure time of one hour, at a PRF = 4 Hz, N = (4)(60)(60) = 14,400 pulses are produced. Therefore, the total energy deposited in the load during a one hour exposure is the

$$\text{energy/pulse signal} \cdot \text{\# pulse signals}$$
$$= (0.232 \text{ joules})(14{,}400 \text{ pulse signals})$$
$$= 3.34 \times 10^3 \text{ joules}$$

The average power equals the energy/pulse signal divided by the interpulse period, T.

$$P_{avg} = \frac{\text{energy/pulse signal}}{T} = \frac{0.232 \text{ joules}}{0.25 \text{ sec}} = 0.928 \text{ watts}$$

This low value of average power, in comparison to the peak power, is due to the very low duty factor of the pulse signal. Note that we are taking into consideration all components of the pulse signal for the purposes of this discussion, so we will define τ^* where τ^* equals the entire time duration of the pulse signal. From Figure 4.5, τ^* = 240 ns, so the duty factor = $\tau^*/T = 240 \times 10^{-9}/0.25 = 9.60 \times 10^{-7}$. Thus, the equipment, operating at a PRF of 4 Hz, has a duty factor of 0.000096%.

The power spectrum for an individual pulse signal can easily be determined from Figure 4.6. The peak voltage amplitude for the frequency spectrum was found to be V = 5.45×10^{-3} V. Thus, the peak amplitude for the power spectrum is

$$P = \frac{V^2}{R} = \frac{(5.45 \times 10^{-3})^2}{63} = 4.72 \times 10^{-7} \text{ watts} = 0.472 \ \mu w$$

The envelope of the power spectrum is shown in Figure 4.10. Found within this envelope, at intervals of 4 Hz, are the spectral lines. The area under these spectral lines equals energy; thus, the total area under all the spectral lines is equal to the total energy of the pulse signal.

From Figure 4.10 it can be seen that the vast majority of the power is located at frequencies less than 25 MHz, and that for frequencies above 100 MHz, the power is essentially zero. In the next chapter, this will become useful when the impedance of the cell holder is measured over the frequency range of 1 MHz to 100 MHz.

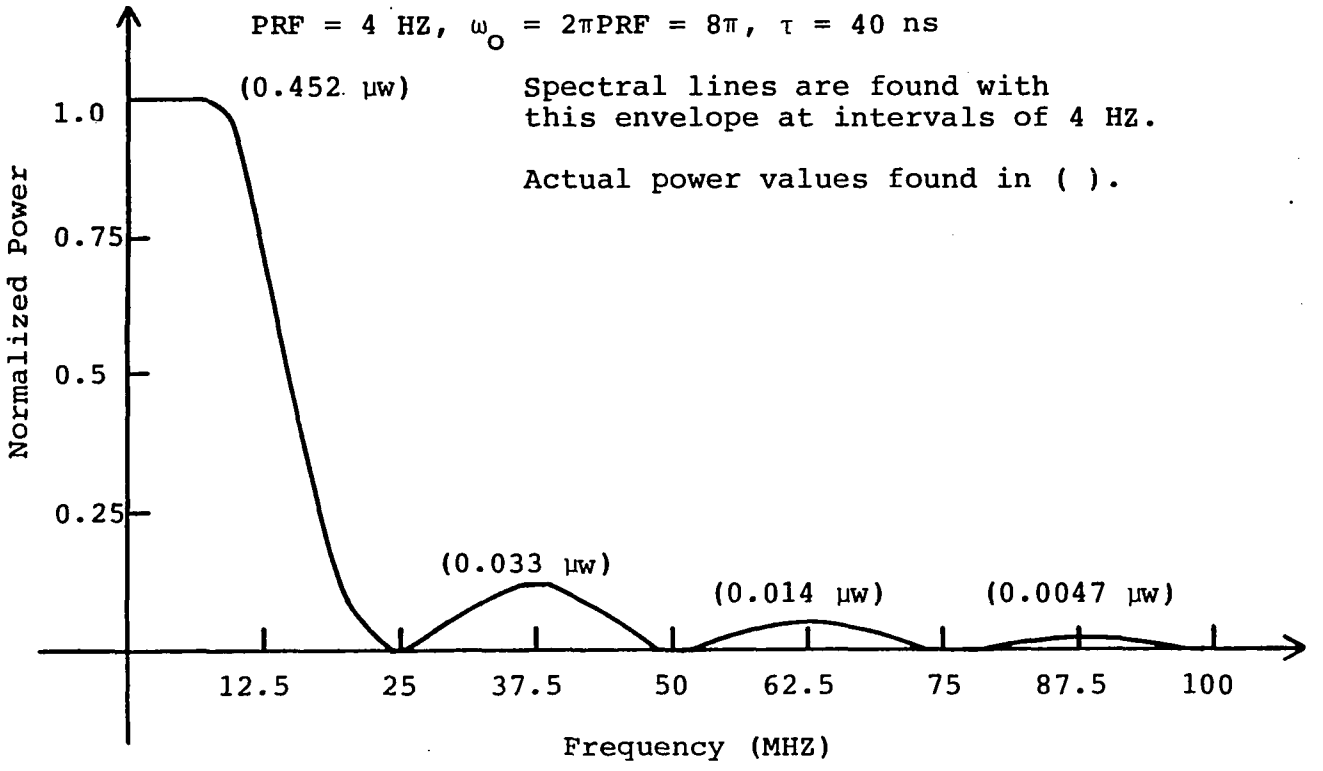

Figure 4.10. Power spectrum envelope for the mismatched termination (actual case).

CHAPTER 5

CELL HOLDER ANALYSIS

Before the electric field strength within the parallel-plate cell holder can be determined, the actual filled cell holder impedance must be found. This will be measured on a vector impedance meter, and then compared to the calculated impedance value based on the measured value of medium conductivity.

Parallel-Plate Cell Holder Impedance

In Chapter Three, the impedance of the filled parallel-plate cell holder (referred to hereafter as simply the "cell holder") was calculated to be approximately 75 ohms. New teflon disks were machined to the dimensions shown in Figure 3.2, thereby yielding this cell holder impedance of 75 ohms. This value of 75 ohms was based on the calculated value for conductivity, determined from the impedance measurements of Dr. Jones's cell holder, listed in Table 3.1.

When the new teflon disks were completed, the impedance of the new cell holder was measured with a Hewlett Packard, Model 4815A, RF Vector Impedance meter. The results of these measurements are shown in Table 5.1. For frequencies less than 25 MHz, the impedance is essentially

Table 5.1. Filled cell holder impedance measurements.

Frequency (MHz)	Magnitude	Phase	Impedance
1	66	0	66.00 + j0.00
2	66	0	66.00 + j0.00
4	64	0	64.00 + j0.00
6	64	0	64.00 + j0.00
8	64	0	64.00 + j0.00
10	63	0	63.00 + j0.00
12	63	0	63.00 + j0.00
14	63	0	63.00 + j0.00
16	62	0	62.00 + j0.00
18	64	0	64.00 + j0.00
20	63	-1	62.99 - j1.10
22	61	-2	60.96 - j2.13
24	62	-2	61.96 - j2.16
26	62	-2	61.96 - j2.16
28	63	0	63.00 + j0.00
30	62	-2	61.96 - j2.16
32	61	-2	60.96 - j2.13
34	63	-2	62.96 - j2.20
36	60	-2	59.96 - j2.09
38	59	-2	58.96 - j2.06
40	61	-2	60.96 - j2.13
42	58	-2	57.96 - j2.02
44	60	-1	59.99 - j1.05
46	62	0	62.00 + j0.00
48	60	0	60.00 + j0.00
50	59	0	59.00 + j0.00
55	59	0	59.00 + j0.00
60	60	0	60.00 + j0.00
65	60	0	60.00 + j0.00
70	58	0	58.00 + j0.00
75	57	0	57.00 + j0.00
80	56	0	56.00 + j0.00
85	57	0	57.00 + j0.00
90	57	+1	56.99 + j0.99
95	58	+2	57.96 + j2.02
100	57	+3	56.92 + j2.98

real, and has an average value of approximately 63 ohms. The reason that this varies from the expected value of 75 ohms may be seen by looking at the measured values for medium conductivity.

Medium Conductivity

The following measurements were made with a conductance meter, type CDM2e, produced by Radiometer A/S Copenhagen. The meter measured conductance over a path length of 0.62 cm. The measurements taken are shown in Table 5.2. RPMI, in Table 5.2, represents RPMI 1640 medium, which is a commercially available solution (see Appendix A for component listing) used to maintain cell cultures. The medium used for maintaining the L1210 mouse leukemia cell line, is a mixture of RPMI 1640 plus 20% fetal calf serum (FCS). Hence, the measured electrical conductivity value for RPMI with 20% FCS is 12.097 mmho/cm. The 2:2 mixture, in Table 5.2, represents a mixture of 2 ml of RPMI 1640 with 20% FCS and 2 ml of distilled water. The 1:3 mixture, likewise, represents a mixture of 1 ml RPMI 1640 with 20% FCS and 3 ml distilled water.

The conductivity of these mixtures were measured, in an attempt to see if the cell holder impedance could be increased to the point where it matches the characteristic impedance of the transmission line. Cell holder impedance

Table 5.2. Solution conductivity measurements.

Solution Measured	Conductivity (mmho/cm)
0.1 N KCL	7.5/0.62 = 12.097
0.9% NaCl	8.6/0.62 = 13.871
RPMI	8.0/0.62 = 12.903
RPMI with 20% FCS	7.5/0.62 = 12.097
2:2	4.1/0.62 = 6.613
1:3	2.6/0.62 = 4.194

and medium conductivity are inversely related by the following expression:

$$Z = \frac{d}{\sigma A}$$

where, Z = the impedance of the cell holder

d = the distance between the parallel plates

A = the area of one plate = πr^2

σ = the conductivity of the medium between the plates

r = the radius of the metal plate

Thus, the impedance of the holder can be increased by decreasing the conductivity of the medium. But, it was believed that in changing the conductivity enough to match the impedance, the resulting diluted medium might have an adverse effect on the cells. The mismatch analysis in the last chapter demonstrated that the pulse magnitude is not appreciably affected by the termination mismatch resulting when the medium's conductivity is unaltered, i.e. σ = 12.097 mmho/cm. Therefore, it was decided that it would be best to keep the cell medium unchanged, and accept the termination mismatch.

Calculating the cell holder impedance based on the measured value of cell medium conductivity, yields

$$Z = \frac{1.5}{(12.097\text{x}10^{-3})\pi(0.772)^2} \cong 66 \text{ ohms}$$

This is much closer to the measured values of cell holder impedance, found in Table 5.1, than the initial calculated value of 75 ohms.

Parallel-Plate Cell Holder E-Field

The electric field strength within the parallel-plate cell holder can easily be determined from the potential drop across the holder. In chapter four, Figure 4.2, there is a graph showing maximum pulse magnitude versus pulse repetition frequency. The higher the PRF, the lower the resulting pulse magnitude. This pulse magnitude is the potential drop across the cell holder. The plate separation in the cell holder is 1.5 cm, so the electric field strength between these plates is:

$$|\underline{E}| = \frac{\text{maximum pulse magnitude}}{1.5 \text{ cm}}$$

Equation 4.2, which relates ideal maximum pulse magnitude to PRF, can be altered to show the actual electric field strength, based on resultant PRF, due to the termination mismatch. The maximum pulse magnitude, with the termination mismatch is:

$$50 \text{ KV} \cdot \frac{63}{63+80} = 22.03 \text{ KV}$$

Therefore,

$$E = \frac{22.03 \text{ KV}}{1.5 \text{ cm}} \quad [1 - \exp(-1/0.126 \text{ PRF})]$$

This equation can be put into graphical form, allowing an easy determination of parallel-plate E-field based on obtained PRF. See Figure 5.1.

From Figure 5.1, it can be seen that for a PRF = 4Hz, the E-field within the parallel-plate cell holder is found to be, E = 12.67 KV/cm.

Energy Deposition in the Parallel-Plate Cell Holder

In Chapter Four, the peak signal power was found to be,

$$\text{Ppeak} = \text{IV} = 5.73 \text{ MW}$$

and the energy per pulse to be,

$$0.232 \text{ joules.}$$

The transmission line is used, in this application, to form a pulse of a specific duration, dependent on the length of the line. The pulse which is formed appears across the load (the cell holder). Thus, the peak power through the cell holder = Ppeak = 5.73 MW, and the total amount of energy deposited in the cell holder per pulse signal is identically

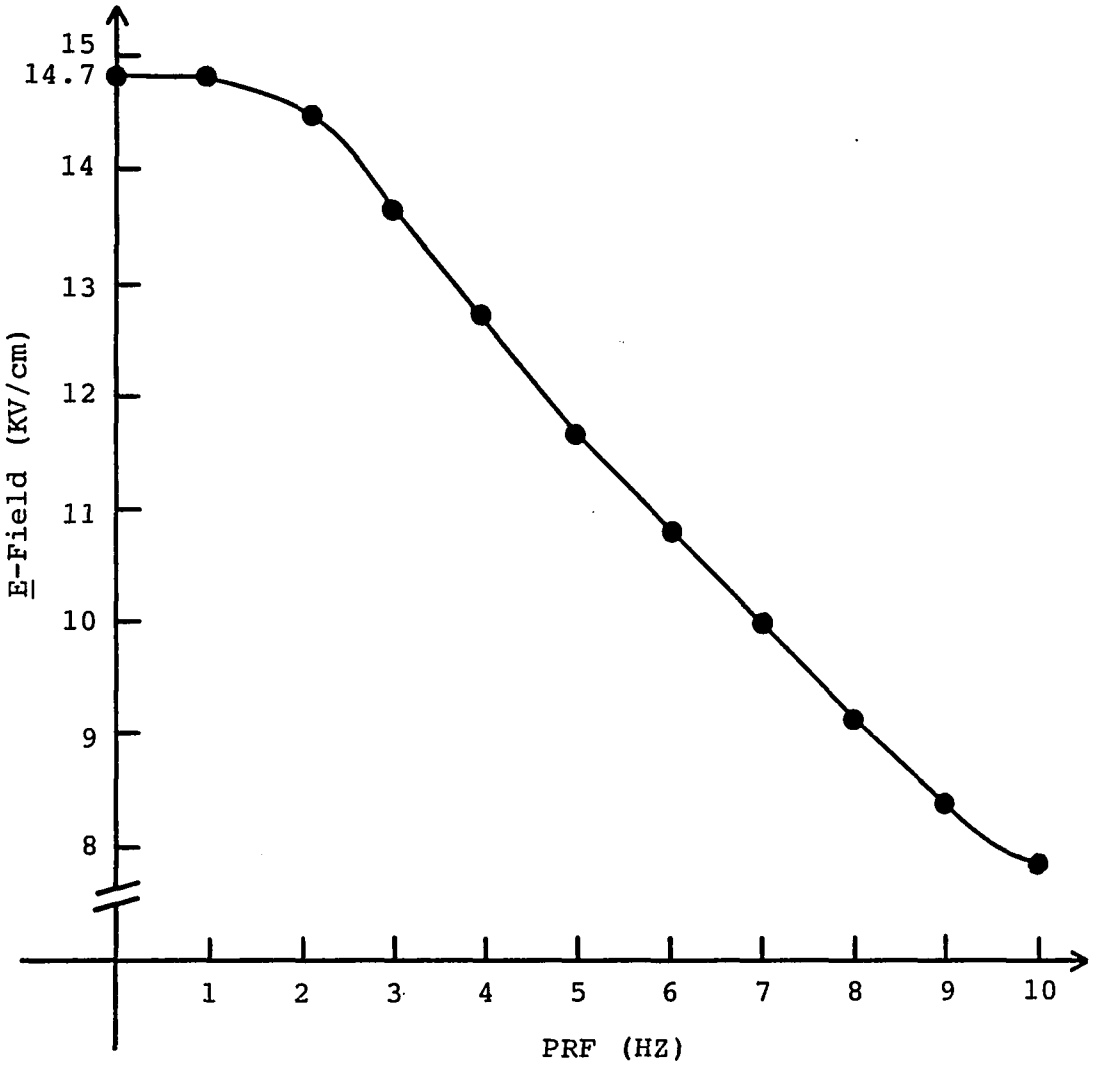

Figure 5.1. Electric field within the cell holder versus obtained PRF.

equal to the energy per pulse signal. (The "pulse signal" is that 240 ns segment consisting of six pulses.)

Energy deposited in the cell holder =

0.232 joules = 0.0554 calories

For a two hour exposure, at a PRF = 4 Hz, that would imply that the total energy deposited is:

Total Energy Deposited for 2 Hour Exposure

= 0.232 joules/pulse · (4)(60)(120) pulses

$= 6.682 \times 10^3$ joules

$= 1.596 \times 10^3$ calories

But, during each pulse signal, this energy is deposited in 240 ns, and there is a delay of approximately 0.25 seconds before the next pulse signal occurs. During this delay, some of the energy is lost in the form of heat, by conduction. The deposited energy causes the temperature of the cell solution to rise. This establishes a thermal gradient across the brass plate, of the cell holder, which creates an outward thermal energy transfer.

The total temperature rise in the medium (measured with a Vitek temperature probe), during a two hour exposure, was 1.1°C. The specific heat of water, and approximately that of the RPMI 1640 cell media is 1.000 cal/gm .°C, and the density of water is given to be 1.00 gm/cm^3. For a cell

holder capacity of 2.79 ml, it therefore, takes approximately

$$\frac{1.000 \text{ cal}}{\text{gm} \cdot {}^\circ\text{C}} \cdot \frac{1.00 \text{ gm}}{\text{cm}^3} \cdot \frac{\text{cm}^3}{\text{ml}} \cdot 2.79 \text{ ml} \cdot 1.1{}^\circ\text{C}$$

$$= 3.069 \text{ calories}$$

to raise the temperature within the cell holder 1.1°C. Since the total energy deposited for a two hour exposure is 1.596×10^3 calories, it is obvious that most of this deposited energy per pulse signal is dissipated before arrival of the next pulse signal.

The therapeutic temperature range for hyperthermia treatment is approximately 43°C to 45°C. Since a two hour exposure with the pulse system only raised the temperature from 25.6°C to 26.7°C, any decrease in cell survival, due to treatment exposure, may be attributed entirely to athermal mechanisms.

CHAPTER 6

BIOLOGICAL PROCEDURES AND EXPERIMENTS

Experiment Overview

Three different sets of experiments were performed. The first set tested the parallel-plate cell holders for toxicity, and tested the procedures used in transporting the cell solutions from the hospital to the Quantum Electronics Laboratory, and back to the hospital. I was concerned about the possibility of contamination during transportation. Some problems were encountered, but were later resolved.

The second set of experiments involved pulsing the cell solution (using the aforementioned pulse system) for varying lengths of time. The time exposure ranged from 30 minutes to 120 minutes, and were performed at 30 minute increments. At the end of each exposure, the cells were brought back to the hospital, where a soft agar assay was performed to determine cell survival.

The final series of experiments tested for synergism between pulsing and exposure to cis-diaminedichloroplatinum (II) (cis-DDP). Cis-DDP is a highly toxic drug presently used in chemotherapy. To check for synergism, three different experiments were performed. First, the cells were pulsed for a length of time, and then exposed to cis-DDP.

Next, the cells were pulsed and exposed to cis-DDP simultaneously. Finally, the cells were exposed to cis-DDP and then pulsed.

A wide variety of experiments were performed; therefore, it was decided from the onset to perform each experiment only once, unless some effect was found (i.e. a decrease in cell survival). If an effect was found, then the experiment was performed a total of three times, to determine if the results were statistically significant.

L1210 Cell Line

The cell line used, for the above described experiments, was the lymphocytic mouse leukemia L1210. These cells exhibit a doubling time of 16 hours, and grow as a stationary suspension culture in RPMI 1640 medium, supplemented with 20% fetal calf serum (FCS) plus 1% Pen-Strep. Pen-Strep is a mixture containing the antibiotics penicillin and streptomycin. This is added to the medium to help prevent contamination.

The medium was prepared in sterile 500 ml bottles. Added to each bottle were 400 ml of RPMI 1640, 100 ml of FCS, and 5 ml of Pen-Strep. This medium was kept refrigerated until needed, at which time the temperature was raised to 37°C, using a warm water bath.

Newly prepared medium was tested for contamination. This was accomplished by preparing a mixture of 2 ml medium

plus 2 ml tryptose-phosphate broth, and then incubating for 2 days. Tryptose-phosphate broth is a nutrient rich solution. If no contamination was noticed after two days, then the new medium was considered safe (contamination free) for use.

Twice a week, the cells were subcultured. They exhibit an exponential growth rate, and start to become confluent at an approximate concentration of 2×10^6 cells/ml. Subculturing keeps the cells subconfluent. The cells are diluted down to an approximate concentration of 10^5 cells/ml and then resuspended in new medium. The cell solution was contained in T-75 tissue culture flasks, and kept in an incubator maintained at 37°C in 10% CO_2. The 10% CO_2 is part of a buffer system necessary to maintain the cell solution at a neutral pH (7.2 - 7.6). The caps on the tissue culture flasks were kept loose, during incubation, to facilitate gas exchange.

The cells were counted optically using a Coulter Counter, Model ZF, by Coulter Electronics. A 100 µl sample of cell solution was removed from the T-75 flask and placed into a coulter counter container. Added to the sample were 10 ml of Isoton solution, which maintain the cells in an isotonic environment (i.e. prevents osmotic shrinking or swelling). The container was then placed under a probe, where 0.5 ml of this mixture was sampled. To obtain the concentration of the original 100 µl sample, the readout on

the counter was first multiplied by 100 (to account for the dilution), and then divided by 0.5 (as only 0.5 ml is sampled at a time). This yielded the number of cells per ml in the 100 µl sample. Typically, two counts were taken and then averaged before applying the correction factors.

Soft Agar Assay

After each experiment, a soft agar assay was performed to determine cell survival. The assay was performed in the following manner. Prior to each experiment, 60 mm petri dishes (the number of which was dependent upon the particular experiment) were each filled with 6.5 ml of 0.5% agar medium and then set aside and allowed to harden.

The 0.5% agar medium is a mixture containing 40 ml of 1.25% agar, which was prepared beforehand and refrigerated (see Appendix B for 1.25% agar preparation), and 60 ml of survival mix. The survival mix consists of 40 ml of double strength RPMI 1640 (supplemented with 2% Pen-Strep) and 20 ml FCS. The survival mix, which was also kept refrigerated, was warmed to 45°C in a water bath. The 1.25% agar was then melted in boiling water and transferred to the 45°C water bath. The agar and survival mix were then combined to yield 100 ml of 0.5% agar medium. This medium was kept at 45°C (during the experiment) to keep it from hardening.

After the cells had been treated, they were spun down in a centrifuge, and then resuspended in new medium. The cells were counted, and serial dilutions were performed to obtain a final concentration of 2×10^4 cells/ml (the cells were treated at an approximate concentration of 10^6 cells/ml). A 0.5 ml sample was then removed and added to 1 ml of agar medium. This 1.5 ml mixture, now containing a total of 1×10^4 cells, was added to one of the 60 mm plates, on top of the 6.5 ml of solidified agar. Thus, the dish now contained approximately 1×10^4 cells. After this was done to each petri dish, they were then incubated for seven days at 37°C in 10% CO_2, allowing the cells to replicate into colonies.

After the incubation period, the colonies were then counted, using a microscope, to determine percent survival. Three petri dishes were used for each treatment group. For example, during each pulse experiment, two cell samples where used as controls, and one sample was treated (i.e. pulsed); thus, a total of nine petri dishes were used per pulse experiment.

A grid, which is sectioned into square centimeters, was taped to the bottom of the 60 mm dish to be counted. Using a 4x ocular, the number of colonies in 2 cm^2 were counted. This was then multiplied by two, arriving at the total number of colonies per 4 cm^2. The other two dishes in a particular group were counted in a similar manner. The

three values obtained were averaged and then divided by four to obtain the average number of colonies per cm^2 for that group. The number of colonies/cm^2 was multiplied by 21.24 cm^2/plate (area of 60 mm plate) to obtain the total number of colonies per plate. Dividing the number of colonies counted/plate by the number of cells seeded (originally placed in the dish) yielded the plating efficiency for that group. Ideally, if each cell seeded forms into a colony, then the plating efficiency would be 100%. The above procedure was performed for each control group, and the treatment group. To obtain the percent survival for the treatment group, the plating efficiency of the treatment group was divided by the plating efficiency of the control group.

Toxicity And Transportation Experiments

Before the pulse experiments could be performed, the cell holders needed to be checked for L1210 cell toxicity, and the procedures involved in transporting the cells from the hospital to the Quantum Electronics Laboratory (QEL) and back needed to be tested against the possibility of contamination. The hospital lab is too small for the pulse system to be located there, thus necessitating the transportation of the cells from the hospital to the QEL and back.

The hospital laboratory is equipped with static and laminar flow hoods, in which, the cell solutions can be handled in a somewhat sterile environment. Since the cell

solution would be in the QEL for up to three hours at a time, a static flow hood was constructed, at the QEL, to provide a contamination free environment there. A vented hood was donated by the Microelectronics Laboratory. The vent was blocked off, doors were added to the front, and a 30 watt, ultraviolet germicidal lamp was installed. The uv lamp was kept on at all times (except during an experiment), to maintain a contamination free hood. With this hood in place, at the QEL, the experiments could then take place.

To check the cell holders for L1210 cell toxicity, both holders were placed under a hood, in the hospital. (Prior to every experiment, the cell holders were washed with 70% ethanol, and then dry sterilized, under pressure, at 121°C for 25 minutes). The holders were filled with cell solution (using a syringe equipped with a 1 1/2 inch, 21 gauge needle) at an approximate concentration of 1×10^6 cells/ml. The solution was kept in the holder for 30 minutes and then removed. To extract any cells which may remain in the holder, clean medium was injected into each holder and then removed. This was performed two times. All extracted solution was then combined and spun down. The medium was poured off, and the remaining cells (which had been compacted at the bottom of the centrifuge tube) were resuspended in 3 ml of medium, the original capacity of the cell holder. The cells were then assayed for colony survival in soft agar. The plating efficiency for the control

was 54%, and the average percent survival for the two holders was 97%. Thus, the holders provided a non-toxic environment for the cell solution.

A small insulated cooler was used to transport the cells from one laboratory to the other. In the first attempted transportation to the QEL, the cells were contained within syringes (three separate samples) and placed in the cooler. Upon arrival at the QEL, one cell sample was placed in a centrifuge tube and kept within the hood, to be used as a control. Another sample was injected into one cell holder and placed within the hood to be used as another control. The last sample was placed into the remaining holder and then connected to the transmission line (outside the hood). With the pulse system off, the holder was kept in place for 30 minutes. At the end of 30 minutes, the solutions were removed from both holders and the centrifuge tube. The holders were rinsed twice with clean medium, to remove any remaining cells (as described earlier), and the three samples were brought back to the hospital, in new syringes (contained within the cooler), where a soft agar assay was performed.

After five days of incubation, contamination was noticed on most of the plates, including the controls. The colonies were counted at that time (instead of waiting the full seven days). The plating efficiency was found to be 79%, and the average percent survival for the two cell

holders was 100%. This supports the results of the first experiment, but since contamination was found, the transportation procedures were altered.

Instead of transporting the cells in syringes, the cells were transported in centrifuge tubes with loosened caps. Upon arrival the tubes were shaken, to insure homogeneity, and then flamed using an alcohol burner, within the hood. A syringe was used to transfer the cells from the centrifuge tube to the holders. At the conclusion of the experiment, new syringes were used to transfer the cells back into sterile centrifuge tubes. These tubes were shaken and flamed again before being brought back to the hospital. These new procedures were first performed during the pulse experiments. All subsequent experiments, including the pulse experiments, were found to be contamination free.

Pulse Experiments

Four different experiments were performed; exposure for 30 minutes, 60 minutes, 90 minutes, and 120 minutes. Each experiment was timed using a stopwatch. To determine the average pulse repetition frequency, the PRF was sampled several times during an experiment, and the results averaged. Each sampled PRF was determined by dividing 100 by the length of time required for 100 pulses. The spark gap was not triggered, so the PRF was not constant during an experiment. This sampling method provided an approximate

determination of the average PRF. Using this value for PRF, the average electric field strength within the holder could be determined using the graph in Figure 5.1. The results of these four experiments are given in Figure 6.1.

The first experiment performed was for a 30 minute exposure. No significant decrease in cell survival was observed, in comparison to the control plating efficiency; therefore, the exposure time was lengthened by 30 minutes in the next experiment. No significant decrease in cell survival, relative to the controls, was noticed in each subsequent experiment. An exposure time greater than two hours was considered impractical, so the incremental increase in exposure time was terminated at that point.

Each experiment utilized two controls. One control was a cell sample contained in a centrifuge tube kept in the QEL hood, and the other was a cell sample contained in the spare cell holder, also kept within the hood. The plating efficiency for these controls were averaged, and this value was divided by the plating efficiency for the treatment sample to determine the treatment group percent survival.

If the average plating efficiency, for a particular experiment, was found to be over 100%, then this value was taken to be 100%. If a plating efficiency of over 100% was used in calculating the percent survival, then the possibility existed that this could give a false indication of a positive treatment effect (because, the treatment sample

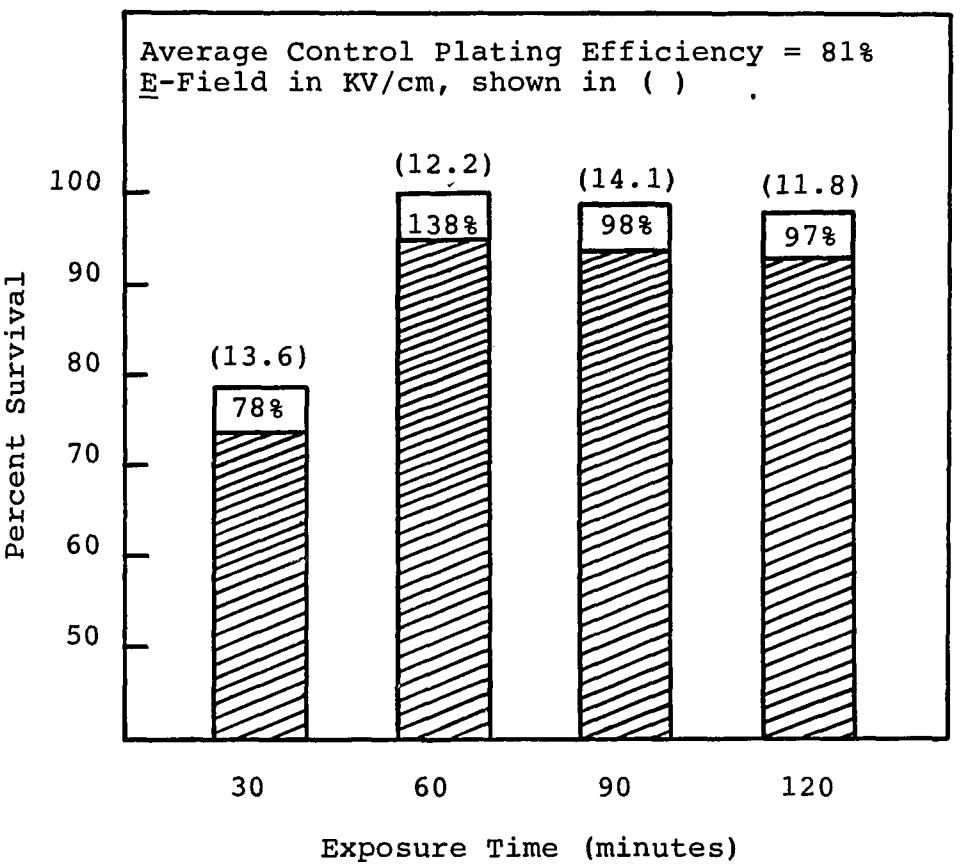

Figure 6.1. Results of the four pulse experiments.

plating efficiency is divided by the control plating efficiency to determine percent survival).

When counting colonies, the likelihood of counting the same colony more than once (and obtaining an overly high plating efficiency) is far greater when there are a large number of colonies present than when a small number of colonies are present. This is also the probable reason for the overly high percent survival (138%) found for the 60 minute pulse experiment, shown in Figure 6.1.

Although pulsing had no effect on cell survival, the possibility of synergism with a chemotherapeutic drug was investigated. Due to its availability, cis-diaminedichloroplatinum (II), was chosen.

Cis-Diaminedichloroplatinum (II) (Cis-DDP)

Cis-DDP is an inorganic heavy metal complex containing a central atom of platinum surrounded by two chloride atoms and two ammonia molecules in the cis position. Its molecular formula is Pt $Cl_2H_6N_2$, and it has a molecular weight of 300.1 grams/mole. Figure 6.2 shows the structural formula. It is soluble in water or saline at 1 mg/ml, and in dimethylformamide at 24 mg/ml.

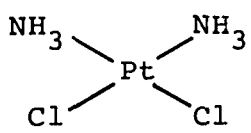

Figure 6.2. Cis-diaminedichloroplatinum (II) structural formula.

Cis-DDP is commercially produced by the Bristol-Myers Oncology Division under the name Platinol. It is a cancer chemotherapeutic agent currently being administered as treatment for metastatic testicular tumors, metastatic ovarian tumors, and advanced bladder cancer. In the treatment against metastatic testicular tumors, combination therapy is employed, where cis-DDP is combined with bleomycin sulfate and vinblastine sulfate. In metastatic ovarian tumors, cis-DDP is combined with doxorubicin. Cis-DDP is used as a single agent in patients with transitional cell bladder cancer no longer amenable to surgery or radiotherapy. The cytotoxic action of cis-DDP is believed to be due to chromosome aberrations, such as the production of DNA interstrand and intrastrand crosslinks.

Cis-DDP has the potential to produce several adverse reactions. Nephrotoxicity (i.e. affecting the kidney) is the major dose limiting toxicity. The impairment of renal function is associated with renal tubular damage. Hypersensitivity can also occur producing anaphylactic-like reactions (for example, facial edema, broncho-constriction, and hypotension). This can occur within minutes of administration to patients with prior exposure to cis-DDP. Ototoxicity has also been observed. It is manifested by tinnitus (noise in the ear, such as ringing) or hearing loss in the high frequency range of 4 KHz to 8KHz.

Synergism Experiments with Cis-DDP

In checking for synergism with cis-DDP, three different types of experiments were performed. First, the cells were exposed to cis-DDP at a concentration of approximately 6.5 μM, for one hour and then pulsed for one hour. Next, the cells were first pulsed for one hour and the exposed to cis-DDP at 6.5 μM. Finally, the cells were exposed simultaneously to pulsing and cis-DDP at 6.5 μM for one hour. The particular concentration of cis-DDP used, 6.5 μM, and the time exposure of one hour were chosen as it produces approximately 50% survival in the L1210 cell line. The pulse time duration was arbitrarily chosen to coincide with the drug exposure time duration.

The cells were exposed to cis-DDP in a centrifuge tube incubated at 37°C in 10% CO_2. Prior to each synergism experiment, 0.00195 grams of cis-DDP were dissolved and mixed into 10 ml of double distilled water to form a 10 ml 0.65 mM cis-DDP stock solution (see Appendix C for stock solution preparation procedures). To expose the cells to the proper concentration of 6.5 μM, a sample, resulting in a 1:100 dilution, is removed from the stock cis-DDP solution and added to the cell solution to be treated. For example, if there were 3 ml of cell solution to be treated, then a 30 μl sample was removed from the stock cis-DDP solution and added to the cell solution, thus diluting the drug sample by a factor of 100, yielding a final concentration of 6.5 μM.

After the drug was added to the cell solution, the centrifuge tube was then placed in the incubator for one hour.

At the conclusion of one hour, the cell solution was removed from the incubator, and the drug treatment terminated by centrifuging the cells and then washing them in prewarmed medium, a total of three times. This removed all traces of cis-DDP from the cell sample.

The results of this series of experiments, including a 60 minute pulse only experiment (for comparison) is shown in Figure 6.3.

The pulse during cis-DDP experiment, and the pulse after cis-DDP experiment, displayed no significant difference in percent survival from that of the cis-DDP control, but the pulse before cis-DDP experiment demonstrated a significant decrease in percent survival compared against the cis-DDP control. Note, each synergism experiment used a cis-DDP control. The cis-DDP control bar, shown in Figure 6.3, represents the mean percent survival of all those individual cis-DDP controls.

The pulse before cis-DDP experiment was performed a total of three times to determine if the results were consistent. The 27% survival, given in Figure 6.3, is the mean percent survival for the three experiments performed. The mean percent survival for the cis-DDP controls, used in those three experiments, was 53%. The standard error is given as:

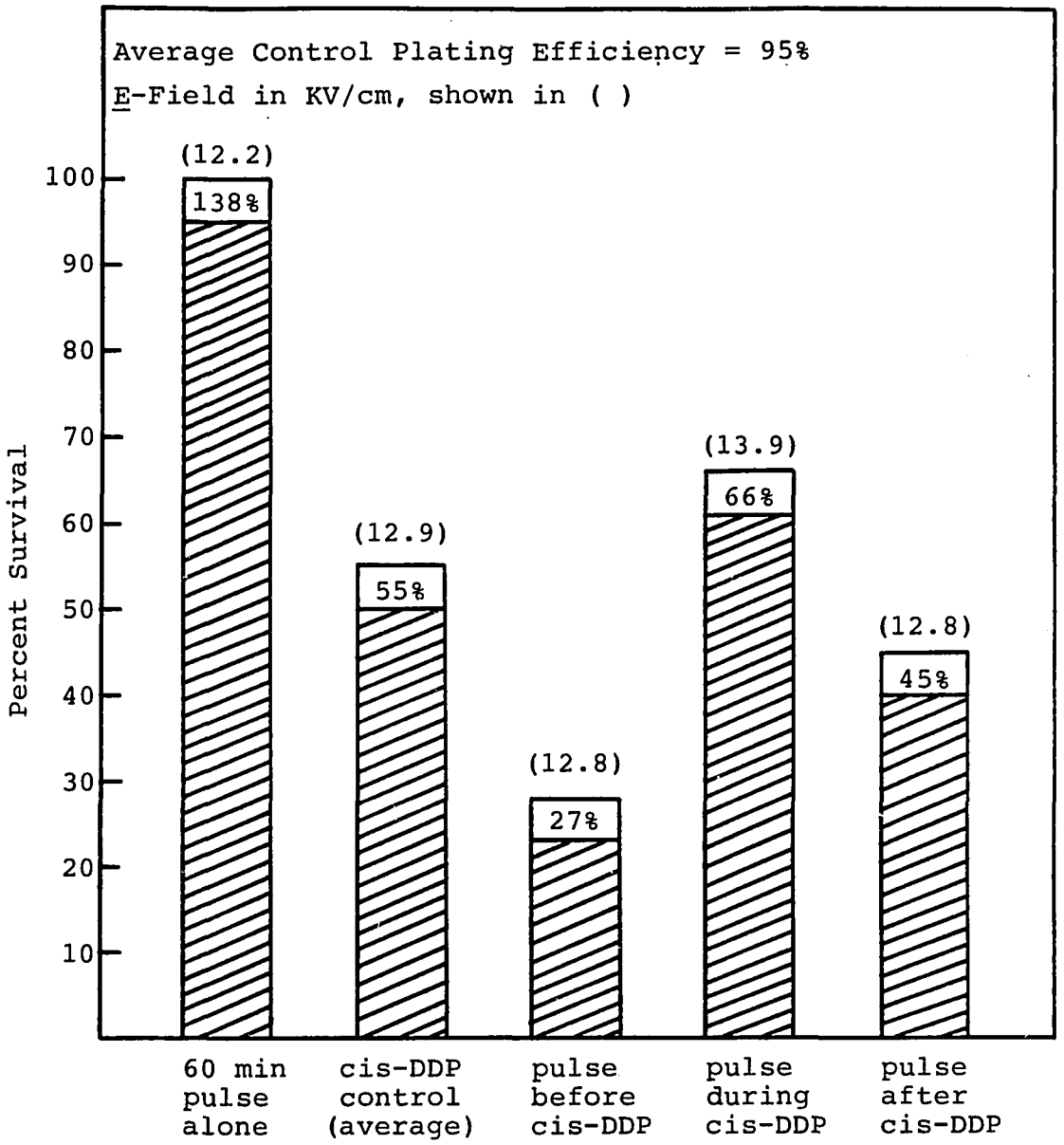

Figure 6.3. Results of the synergism experiments with cis-DDP.

$$s_{\bar{x}} = \sqrt{\frac{\sum x^2}{n(n-1)}}$$

where, x = (the individual value - the mean) = $(X - \bar{X})$

n = the number of experiments performed

For $n = 3$, and a mean of $\bar{X} = 27\%$, the treatment group has a standard error of $s_{\bar{x}} = 0.882$. The range for a 99% confidence interval around the sample mean, is given to be

$$\bar{X} + 2.58\ s_{\bar{x}}$$

Thus the 99% confidence interval around the treatment sample mean is $27 \pm (2.58)(0.882)$ or 25% to 29%. Likewise, for the cis-DDP control, the standard error is calculated to be $s_{\bar{x}} = 2.89$, and the 99% confidence interval around the cis-DDP control sample mean, is 46% to 60%. The treatment sample range is clearly outside of the control cis-DDP sample range, thus indicating a definite synergistic effect when pulsing is performed before exposure to cis-DDP (this is statistically significant for $\alpha = 0.01$).

CHAPTER 7

CONCLUSION

Result Summary

The synergistic effect found, when pulsing occurred before exposure to cis-DDP, appears to be the first positive result obtained with DC pulses having a duration in the nanosecond range! Sandler (Sandler et al., 1974) performed studies on nerve tissue using pulse widths of a fraction of a nanosecond, but obtained negative results.

Killing of microorganisms has occurred when pulses in the microsecond range have been employed. Sale and Hamilton (1967a) performed experiments on bacteria and yeast using 20 μs DC pulses, with field strengths ranging up to 25 KV/cm. The lethal effects they observed were attributed to an irreversible loss of the cell membrane's function as the semipermeable barrier between the cell and its environment. These effects were believed to be due to DC pulse treatment, and not to any thermal mechanism.

The significant decrease in cell survival, when the cells were pulsed prior to cis-DDP exposure, is probably due to increased permeability of the cell membrane, thus allowing greater drug uptake than normal. Since pulsing alone had no significant effect upon cell survival, it is

reasonable to assume that any change in cell membrane permeability is either reversible, or not significant enough to adversely affect the cell's survival.

Sale and Hamilton (1968) observed that cell lysis occurred when the potential difference aross the membrane reached about one volt (using 20 μs pulses). For a spherical cell, they obtained the following equation relating potential difference across the membrane (V) to the electric field strength (E) and the cell radius (a).

$$V = 3/2\ aE$$

Assuming the L1210 to be spherical, with a cell radius of 2 x 10^{-3} cm and a field strength of E = 13 KV/cm, the potential across the L1210 cell membrane is approximately 40 volts. Sale and Hamilton observed 10% survival (1967a), for 10 pulses of 20 μsec width and E ≅ 13 KV/cm (resulting in approximately 1 V across the cell membrane). As 100% survival was observed in the present experiment, for 14,400 pulses (1 hr exposure at a PRF = 4 Hz) of 40 ns width, and E ≅ 13 KV/cm (implying 40 V across the membrane), it is obvious that pulse width is a dominant factor in determining pulsed DC field effects on cell survival.

Even though pulsing alone did not create any significant decrease in cell survival, it appears that field strengths in the range of 12 KV/cm to 15 KV/cm are at the threshold of causing cell membrane aberrations for 40 ns

pulses. This is evidenced by the synergistic effect found in pulsing before cis-DDP exposure. It seems probable that increasing the field strength, beyond that presently available, would result in lethal effects due to pulsing alone.

The importance of investigating the effects of short pulses (nanoseconds) versus longer pulses, lies in the absence of temperature rise in the cell suspension. Treating cells with short pulses clearly yields an insignificant temperature rise (1.1°C for a two hour treatment). This is not the case for longer pulses. In Sale and Hamilton's experiments (1967a), using 20 μs pulses, subhyperthermic temperatures were maintained only by circulating water through the cell holder. Even then, temperature rises of 5 to 10°C were observed. No such cooling mechanism was required for the present system.

Using AC electric fields to induce heating, within a tumor, has been extensively studied. The focus of this work was to explore the possibility of inducing non-thermal electric field effects for in vitro cell solutions. Using nanosecond pulses, experimentation can more readily be extended to the in vivo domain. The absence of a cooling mechanism to maintain subhyperthermic temperatures, as well as an essentially zero DC component, makes this possible.

Future Considerations

The intention of this work was not to perform an exhaustive study of athermal, high power in vitro effects, but rather to investigate the possibility that such effects may exist. When the experiments were initiated, it was unknown what effect, if any, would be observed using short pulses, so a broad range of experiments were performed. Now that some effect has been found, this work can be used as a launching point for a more in-depth, exhaustive study.

Many more experiments can be performed using the present pulse system. For example, now that it has been shown that pulsing for one hour prior to cis-DDP exposure yields a synergistic effect, experiments can be performed to see how time dependent this phenomenon is. Different endpoints can be investigated. Instead of just assaying for cell survival, more sophisticated biological experiments can be undertaken to determine more precisely the effects upon the cell membrane. These are just some examples; many other possibilities exist.

It appears though that continued search for effects due to pulsing alone, using the present pulse system, may be a dead end. But with the relatively inexpensive purchase of a new high voltage DC supply (capable of, for example, 100 KV or higher), a new series of pulse experiments could be performed. Given the higher electric field strength which

would result, it is reasonable to assume that pure pulse effects may be found.

Short pulse, athermal experiments could also be extended to the in vivo domain, where the possibility of using this modality as a form of cancer treatment can be thoroughly investigated. Initially, small parallel-plate reservoirs (filled with conducting fluid) could be constructed in which a tumorous limb may be immersed for treatment. In the future, the design of probes, allowing the treatment to be performed at a more exact location, could be investigated.

Aside from its possible implications in cancer research, high voltage, DC pulsed fields have already been used successfully in cell electrofusion. CW electric fields, of frequency 500 KHz, and field strength 200 V/cm are used to create the formation of pearl chains. Once the cells are aligned, fusion is induced by DC pulses of 600 V/cm and 15 μs duration. Cell membrane breakdown occurs in the region of membrane contact. This results in the formation of pores, allowing the intercellular exchange of cytoplasm. The membranes then reseal, forming fused hybrids.

It is clear that pulsed electric fields have proven to be beneficial in biological research. Long pulse AC fields have been used extensively in hyperthermia work, and short pulse DC fields have shown utility in electrofusion. The work presented in this paper, although preliminary, has

shown that athermal electric fields may have advantageous consequences in cancer research. This work should be continued, if the benefits of short pulse athermal electric fields are to be utilized fully.

APPENDIX A

RPMI 1640 COMPONENTS

Component	mg/L
L - Arginine, free base	200.0
L - Asparagine · H_2O	56.82
L - Aspartic acid	20.0
L - Cystine, disodium salt	59.14
L - Glutamic acid	20.0
L - Glutamine	300.0
Glycine	10.0
L - Histidine, free base	15.0
L - Hydroxyproline	20.0
L - Isoleucine	50.0
L - Leucine	50.0
L - Lysine HCl	40.0
L - Methionine	15.0
L - Phenylalanine	15.0
L - Proline	20.0
L - Serine	30.0
L - Threonine	20.0
L - Tryptophan	5.00
L - Tyrosine, 2Na·2H_2O	28.83

Component	mg/L
L - Valine	20.0
p - Aminobenzoic acid	1.0
Biotin	0.20
D - Ca pantothenate	0.25
Choline chloride	3.00
Folic acid	1.00
i - Inositol	35.0
Nicotinamide	1.00
Pyridoxine HCl	1.00
Riboflavin	0.20
Thiamine HCl	1.00
Vitamin B12	0.005
$Ca(NO_3)_2 \cdot 4H_2O$	100.0
KCl	400.0
$MgSO_4$ (anhydrous)	48.84
NaCl	6000.0
Na_2HPO_4 (anhydrous)	800.76

APPENDIX B

1.25% AGAR PREPARATION PROCEDURE

1. For the soft agar assay, it is convenient to prepare 40 ml of agar in 100 ml bottles. Assuming that six bottles are to be prepared, that would imply a total of 240 ml of solution.
2. H_2O density = 1 g/ml; therefore, 240 ml of double distilled water (DD H_2O) implies 240 g of DD H_2O.
3. $x/(240+x) = 0.0125$ for a 1.25% solution, where x = the number of grams of agar $\cong$ 3.04 g.
4. Measure out 3.04 g of bacteriological agar, "Bacto-agar," using the triple beam, or Mettler balance.
5. Mix the 3.04 g agar powder and 240 ml of DD H_2O in a beaker. Heat and stir until thoroughly dissolved.
6. Pour 40 ml of solution into each of the six 100 ml sterilized bottles.
7. Put caps on loosely, and place a strip of sterilizing tape over it. Place the bottles in a metal pan containing about 1/2 inch of water.
8. Sterilize in an autoclave for 15 minutes, or until tape changes color, on liquid cycle only.
9. Let bottles cool overnight before storing in a refrigerator.

APPENDIX C

0.65 mM CIS-DDP STOCK SOLUTION PREPARATION PROCEDURE

1. 10 ml of this stock solution is prepared prior to each syngerism experiment.
2. Molarity is defined as the number of moles of solute per number of liters solution. The molecular weight of cis-DDP is 300.1 g/mole.
3. To prepare 10 ml of stock solution at a concentration of 0.65 mM, the following amount of cis-DDP is required,

$$0.65 \times 10^{-3} \frac{\text{moles}}{\text{liter}} \cdot 300.1 \frac{\text{g}}{\text{mole}} \cdot \frac{\text{liter}}{1000 \text{ ml}} \cdot 10 \text{ ml}$$

$$= 0.00195 \text{ g}$$

4. Measure out approximately 0.00195 g of cis-DDP. Obtaining the exact amount is difficult. Measure out as closely as possible, and then recalculate to determine the precise concentration, based on the actual amount measured.
5. Mix the cis-DDP with 10 ml of DD H_2O in a 30 ml flask, within a dark hood (exposure to light renders the drug inactive).

6. Add an appropriate size stir bar; cover the flask opening with parafilm, and then cover the entire flask with aluminum foil.
7. Place the flask on a stir plate, allowing it to stir continuously for one hour.
8. At the end of one hour, remove the solution from the flask (within a dark hood) with a sterile syringe.
9. Attach a Millex-GS sterilizing filter unit to the syringe, and push the solution through it, into a sterile, 12 ml centrifuge tube. The Millex-GS unit is a sterilizing filter for aqueous solutions dispensed with a syringe. It removes all microorganisms, particles and precipitates larger than 0.22 μm.
10. The sterile stock solution is now ready for use.

SELECTED BIBLIOGRAPHY

American Type Culture Collection. ATCC Catalogue of Cell. Lines and Hybridomas. 5th ed. Rockville: American Type Culture Collection, 1985.

Facts and Comparisons. Drug Facts and Comparisons. St. Louis: Facts and Comparisons, 1986..

Fink, Donald G., ed., and Christiansen, Donald, ed. Electronics Engineers Handbook. 2nd ed. New York: McGraw-Hill Book Company, 1982.

Jones, Roger C., and Overgaard, Jens. "An Athermal In Vitro High Power Pulse Epxperiment," Proceedings of the 4th International Symposium on Hyperthermic Oncology. vol. 1: Summary Paper. London: Taylor and Francis LTD, 1984.

Jordan, Edward C., and Balmain, Keith G. Electromagnetic Waves and Radiating Systems. Englewood Cliffs: Prentice-Hall, Inc., 1968.

Kaune, W. T., Frazier, M. E., King, A. J. Samuel, J.E.; Hungate, F. P., and Causey, S. C. "System for the Exposure of Cell Suspensions to Power-Frequency Electric Fields," Bioelectromagnetics 5 (November 2, 1984): 117-129.

Malec, Michael A. Essential Statistics for Social Research. Philadelphia: J. B. Lipppincott Company, 1977.

Medical Economics Company Inc. Physicians' Desk Reference. 39th ed. Oradell: Medical Economics Company Inc., 1985.

Metzer, Georges, and Vabre, Jean-Paul. Transmission Lines with Pulse Excitation. New York: Academic Press, Inc., 1969.

Middleton, Robert G. Pulse Circuit Technology. Indianapolis: Howard W. Sams and Co., 1964.

Moskowitz, Sidney and Racker, Joseph. Pulse Techniques. Englewood Cliffs: Prentice-Hall, Inc., 1951.

Ramo, Simon, Whinnery, John R., and Van Duzer, Theodore. Fields and Waves in Communication Electronics. New York: John Wiley and Sons, 1984.

Sale, J. H., and Hamilton, W. A. "Effects of High Electric Fields on Microorganisms; I. Killing of Bacteria and Yeasts," Biochimica et Biophysica Acta 148 (July 1967a): 781-788.

Sale, J. H., and Hamilton, W. A. "Effects of High Electric Fields on Microorganisms; II. Mechanism of Action of the Lethal Effect," Biochimica et Biophysica Acta 148 (July 1967).

Sale, J. H., and Hamilton, W. A. "Effects of High Electric Fields on Microorganisms; III. Lysis of Erythrocytes and Protoplasts," Biochimica et Biophysica Acta 163 (March 1968): 37-43.

Sandler, Sheldon S., Smith, Glenn S., and Albert, Ernest N. "Electromagnetic Field Effects in Nerve Tissue," Aviation, Space, and Environmental Medicine 46 (November 1975): 1414-1417.

Stimson, George W. Introduction to Airborne Radar. El Segundo: Hughes Aircraft Company, 1983.

Weast, Robert C., ed. Handbook of Chemistry and Physics. 54th ed. Cleveland: CRC Press, 1973.

Zimmermann, U., and Greyson, J. "Electric Field Induced Cell Fusion," Biotechniques (September-October 1983).

Zimmermann, U. "Cell with Manipulated Functions: New Perspectives for Cell Biology, Medicine and Technology," Angewandte Chemie 20 (1985).